



Institute of High Energy Physics
Chinese Academy of Sciences

Analytic Framework for Neutron Star Critical Masses Across EOS Models in GRBs

July 11, 2025 7^o Galileo Xu-Guangqui meetingGX7



ICRA Net

Rahim Moradi
IHEP-CAS, Beijing, China
rmoradi@ihep.ac.cn



NASA's NICER Tracks a Magnetar's Hot Spots -
NASA SVS

Outline

- ◆ What are the Gamma-Ray Bursts (GRBs)?
- ◆ Evidence of Neutron Star or Black Hole
- ◆ Afterglow Emission: Multipolar emission from highly magnetized NS
- ◆ GRBs, newborn NS, BH, and Afterglow emission (Swift-XRT observation)
- ◆ Dainotti relation and NSs
- ◆ Constraint on Equation of States by afterglow emission of some specific SGRBs?
- ◆ Toward a more complex solution for Afterglow: eccentricity...Model the newborn NS through the equilibrium sequence of Maclaurin spheroids
- ◆ Conclusions

Related Papers

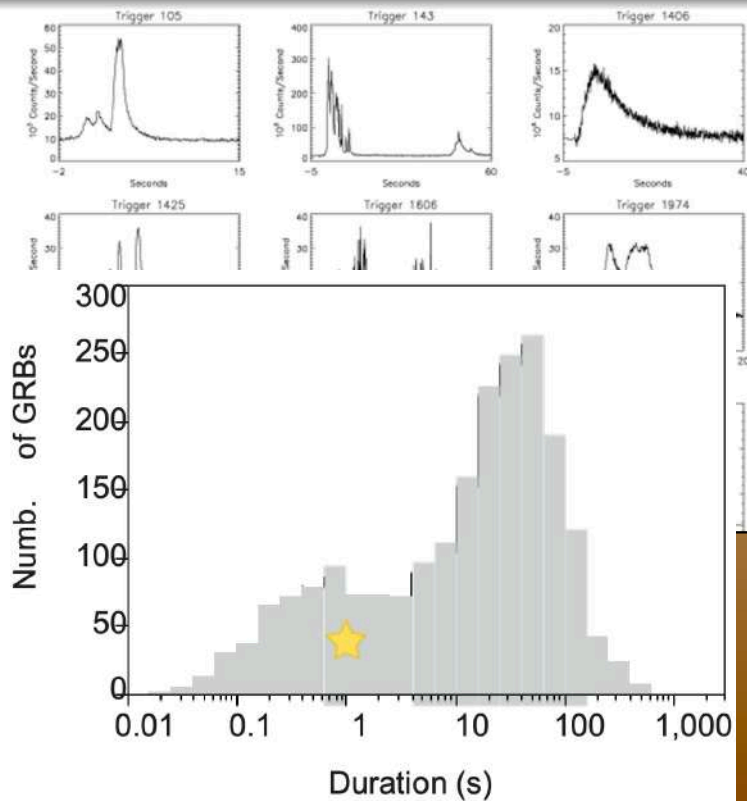
1. Wang, Moradi, Li, The Astrophysical Journal, 974:89 (2024).
2. Rueda, Ruffini, Li, Moradi, Rodriguez, and Wang PRD 106, 083004 (2022).
3. Ruffini, Moradi, Rueda, et al., MNRAS 504, 5301–5326 (2021).
4. Hashemi, Shakeri, Wang, Li, and Moradi, ApJ 986 14 (2025).
5. Moradi, Wang, Rastegarnia, Yorgancioglu, S.X Yi, EslamPanah, S. N. Zhang, et al (2025) (to be submitted).
6. Moradi et al 2024 ApJ 977 155.
7. Emre S. Yorgancioglu, Daban Mohammed Saeed, Rahim Moradi, Yu Wang, e-Print: 2507.09292 [astro-ph.HE] ApJ

Gamma-ray bursts (GRBs)

Gamma Ray bursts are

Extremely energetic explosions!

- The most **Luminous** sources in the universe!
- They produce energy equivalent to ~ 1 solar mass in 1-100 second $\rightarrow \sim 10^{54}$ erg!
- if explosion $< 2s \rightarrow$ SHORT GRB.
- if explosion $> 2s \rightarrow$ LONG GRB.

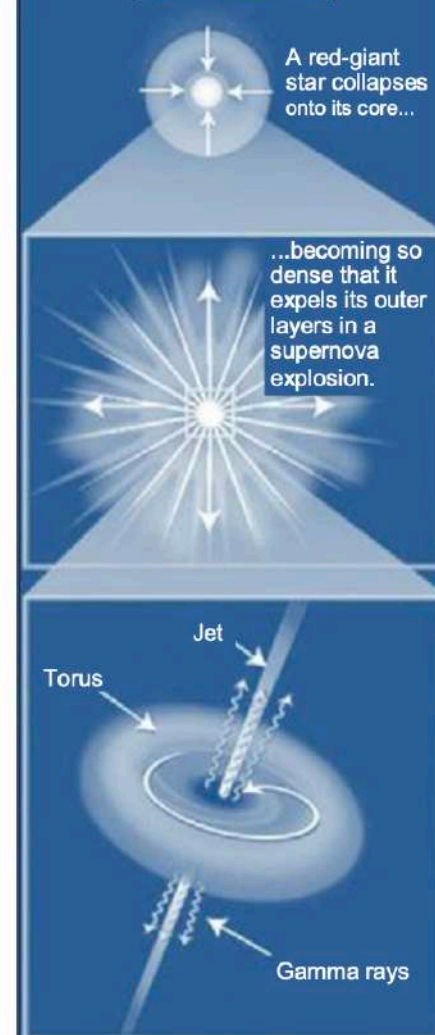


Standard Model of Progenitors

Short gamma-ray burst (<2 s duration)



Long gamma-ray burst (>2 s duration)



1. Radiative Processes of Gamma-Ray Bursts (GRBs): Internal Shock??

Temporal and Spectral Analysis of GECAM Observations

- Study of GRB 230307A: second brightest GRB.
- Temporal behavior, flux evolution, and high-latitude emission.
- Identification of a new subclass (Chen Wei's talk)

Criteria for finding the Long Short GRBs



GECAM

Chen-Wei Wang *et al* 2025 *ApJ* 979 73

A new subclass of gamma-ray burst originating from compact binary merger

Chen-Wei Wang,^{1,2} Wen-Jun Tan,^{1,2} Shao-Lin Xiong,^{1,*} Shu-Xu Yi,^{1,†} Rahim Moradi,^{1,‡} Bing Li,¹ Zhen Zhang,¹ Yu Wang,^{3,4,5} Yan-Zhi Meng,⁶ Jia-Cong Liu,^{1,2} Yue Wang,^{1,2} Sheng-Lun Xie,^{1,7} Wang-Chen Xue,^{1,2} Zheng-Hang Yu,^{1,2} Peng Zhang,^{1,8} Wen-Long Zhang,^{1,9} Yan-Qiu Zhang,^{1,2} and Chao Zheng^{1,2}

¹Key Laboratory of Particle Astrophysics, Institute of High Energy Physics, Chinese Academy of Sciences, Beijing 100049, China

²University of Chinese Academy of Sciences, Beijing 100049, China

³ICRANet, Piazza della Repubblica 10, I-65122 Pescara, Italy

⁴ICRA, Dipartimento di Fisica, Sapienza Università di Roma, Piazzale Aldo Moro 5, I-00185 Rome, Italy

⁵INAF, Osservatorio Astronomico d'Abruzzo, Via M. Maggini snc, I-64100, Teramo, Italy

⁶School of Science, Guangxi University of Science and Technology, Liuzhou 545006, China

⁷Institute of Astrophysics, Central China Normal University, Wuhan 430079, China

⁸College of Electronic and Information Engineering, Tongji University, Shanghai 201804, China

⁹Qufu Normal University, Qufu 273165, China

(Dated: July 3, 2024)

Type I gamma-ray bursts (GRBs) are believed to originate from compact binary merger usually with duration less than 2 seconds for the main emission. However, recent observations of GRB 211211A and GRB 230307A indicate that some merger-origin GRBs could last much longer. Since they show strikingly similar properties (indicating a common mechanism) which are different from

R. Moradi *et al* 2024 *ApJ* 977 155

Temporal and Spectral Analysis of the Unique and Second Brightest Gamma-Ray Burst GRB 230307A: Insights from GECAM and *Fermi*/GBM Observations

R. MORADI,¹ C. W. WANG,^{1,2} B. ZHANG (张冰),^{3,4} Y. WANG (王瑜),^{5,6,7} S.-L. XIONG (熊少林),¹ S.-X. YI,¹ W.-J. TAN,^{1,2} M. KARLICA,⁸ AND S.-N. ZHANG (张双南)^{1,2}

¹Key Laboratory of Particle Astrophysics, Institute of High Energy Physics, Chinese Academy of Sciences, Beijing 100049, People's Republic of China

²University of Chinese Academy of Sciences, Chinese Academy of Sciences, Beijing 100049, China

³Nevada Center for Astrophysics, University of Nevada Las Vegas, NV 89154, USA

⁴Department of Physics and Astronomy, University of Nevada Las Vegas, NV 89154, USA

⁵ICRANet, Piazza della Repubblica 10, I-65122 Pescara, Italy

⁶ICRA, Dipartimento di Fisica, Sapienza Università di Roma, Piazzale Aldo Moro 5, I-00185 Rome, Italy

⁷INAF, Osservatorio Astronomico d'Abruzzo, Via M. Maggini snc, I-64100, Teramo, Italy

⁸Astronomical observatory Belgrade, Volgina 7, 11060 Belgrade, Serbia

(Dated: Received date / Accepted date)

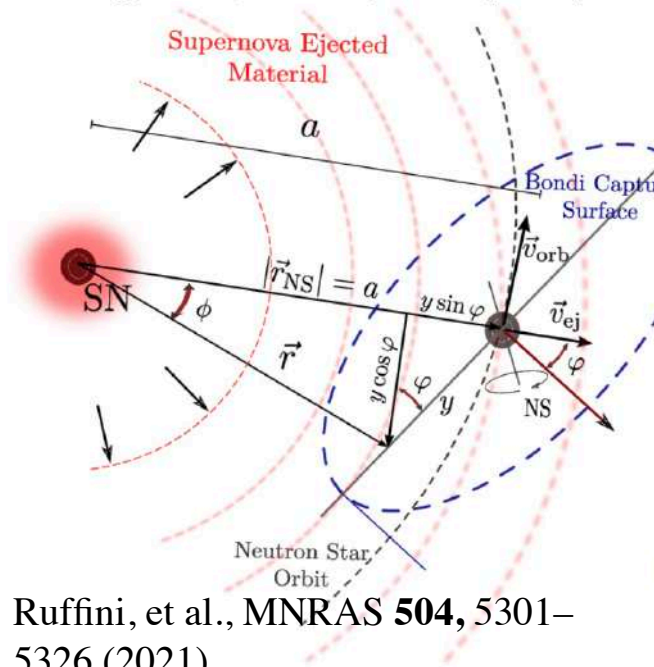
Submitted to *ApJ*

ABSTRACT

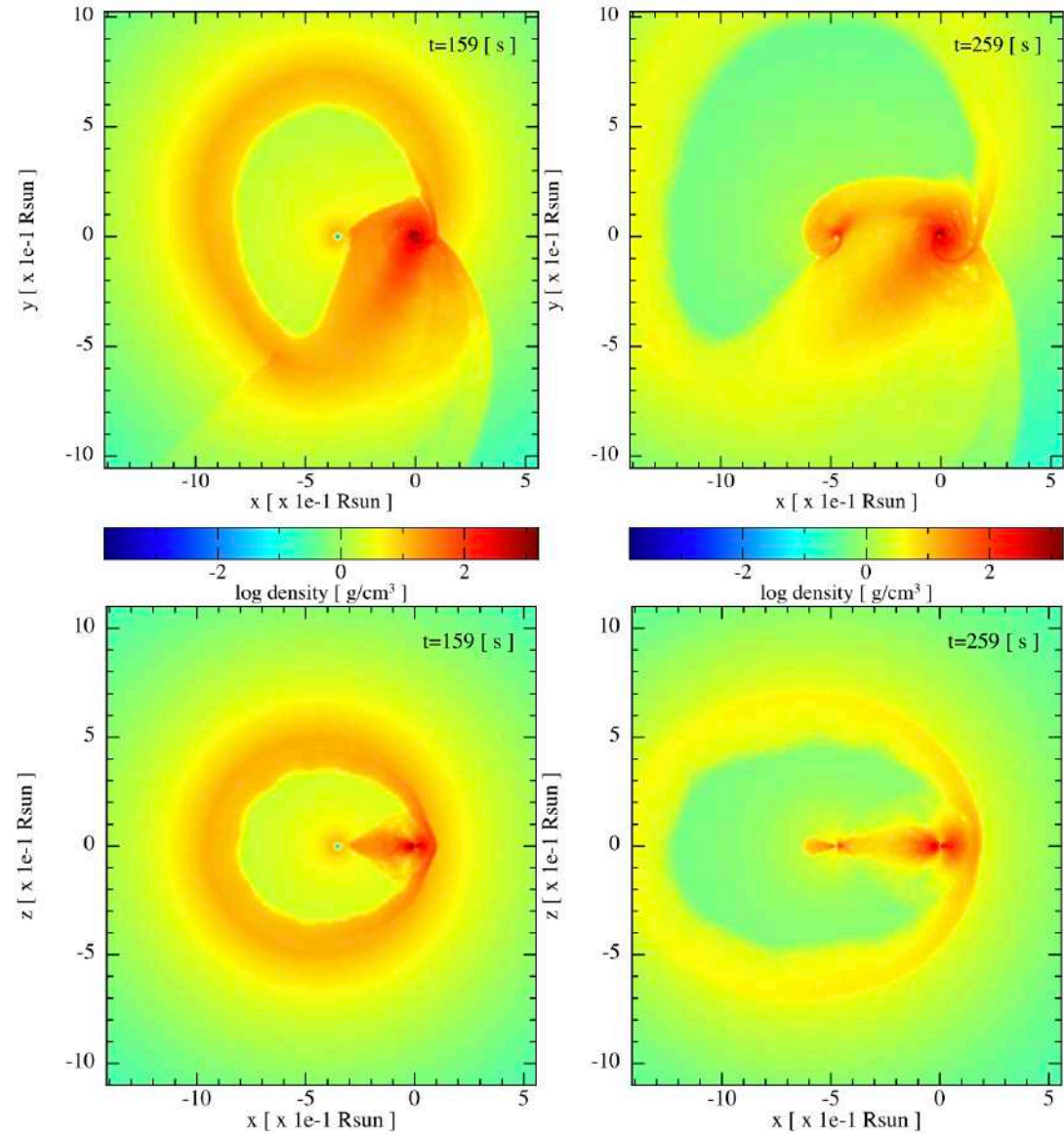
In this study, we present the pulse profile of the unique and the second brightest gamma-ray burst GRB 230307A. and analyze its temporal behavior using a joint GECAM-*Fermi*/GBM time-resolved

(Binary driven Hypernova)

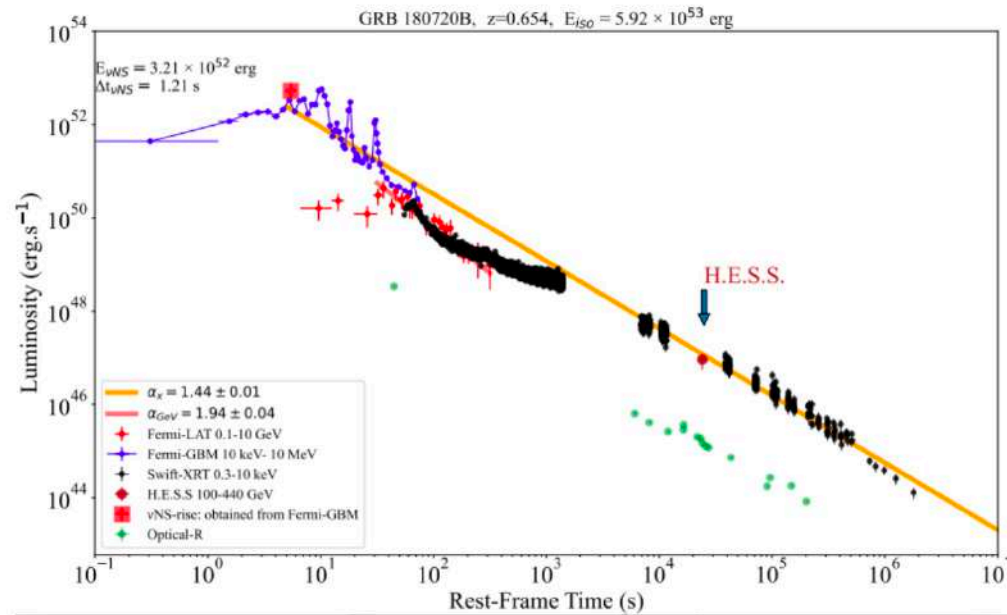
Fryer, et al., ApJ 526, 152 (1999)
Bromberg, et al., ApJ 749, 110(2012)
Götberg, et al., AA 629, A134 (2019)



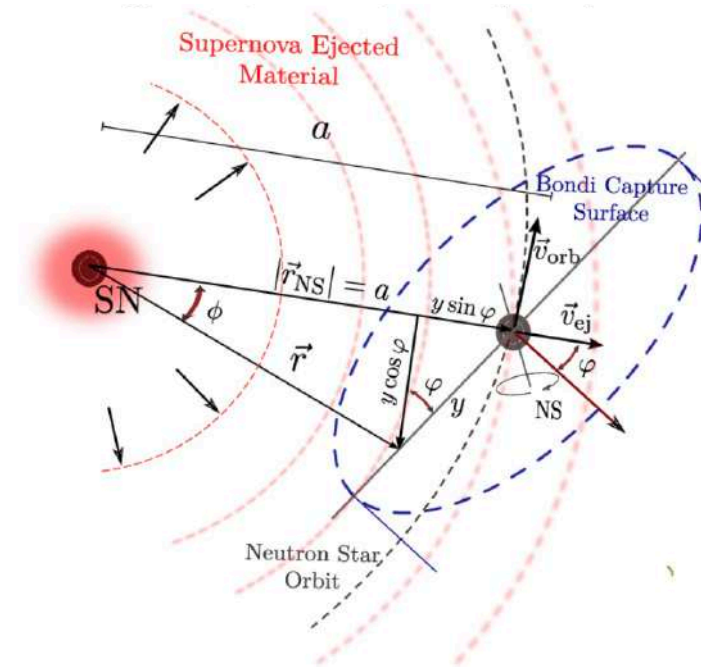
Ruffini, et al., MNRAS **504**, 5301–5326 (2021)
Rueda & Ruffini, ApJ 758, L7 (2012)
Becerra, et al., ApJ 812, 100 (2015)
Becerra, et al., ApJ 871, 14 (2019)



Prompt vs Afterglow in BdHN

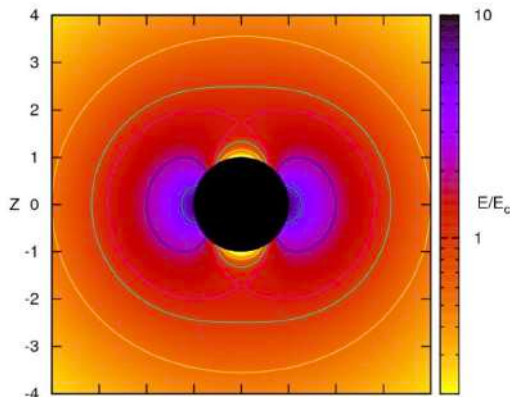
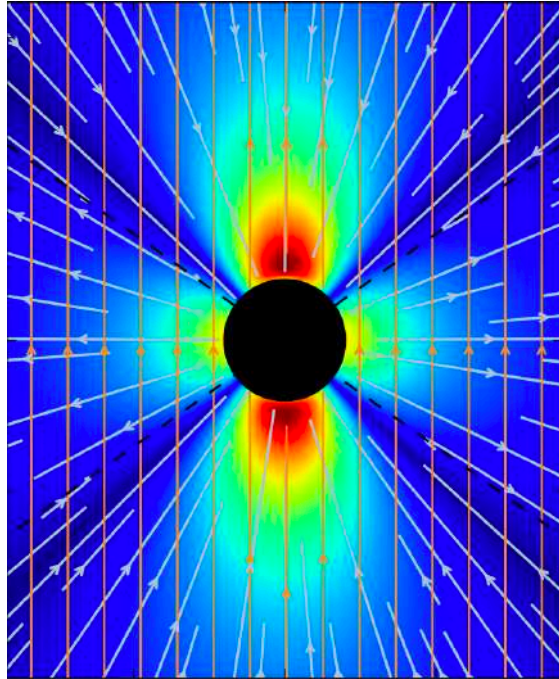


- 180720B
- 18 → 2018
- 07 → July
- 20 → day 20
- B → more than one GRB a day!



Rueda & Ruffini, *ApJ* 758, L7 (2012)
 Becerra, et al., *ApJ* 812, 100 (2015)
 Becerra, et al., *ApJ* 871, 14 (2019)

2. BH + the aligned magnetic field (B0) Moradi et al A&A 2021



Analogy with Kerr-Newmann

Dyadoregion

The dyadoregion energy:

$$E_{(r_+, r_d)} = \frac{(2B_0 JG/c^3)^2}{4r_+} \left(1 - \frac{r_+}{r_d}\right) + \frac{(2B_0 JG/c^3)^2}{4\hat{a}} \times \left[\left(1 + \frac{\hat{a}^2}{r_+^2}\right) \arctan\left(\frac{\hat{a}}{r_+}\right) - \left(1 + \frac{\hat{a}^2}{r_d^2}\right) \arctan\left(\frac{\hat{a}}{r_d}\right) \right], \quad (5)$$

where r_d is the radius of the dyadoregion

$$\left(\frac{r_d}{\hat{M}}\right)^2 = \frac{1}{2} \frac{\lambda}{\mu\epsilon} - \alpha^2 + \left(\frac{1}{4} \frac{\lambda^2}{\mu^2\epsilon^2} - 2 \frac{\lambda}{\mu\epsilon} \alpha^2\right)^{1/2} \quad (6)$$

with $\epsilon = E_c M_\odot G^{3/2}/c^4 \approx 1.873 \times 10^{-6}$, and

$$\lambda = (2B_0 JG/c^3)/(\sqrt{GM}), \quad (7)$$

is the effective charge-to-mass ratio.

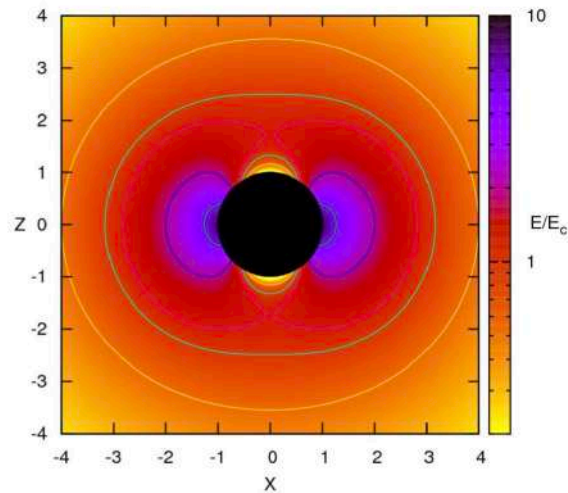
The characteristic width of the dyadoregion, which demonstrates the region in which the electric field around the BH is overcritical is

$$\Delta_d(t) = r_d(t) - r_+(t). \quad (8)$$

Over Critical E field regime and Ultrarelativistic prompt emission phase

Dyadoregion

C. Cherubini et al PRD 79, 124002 (2009)



$E_c = \frac{m_e^2 c^3}{e \hbar}$ is the critical value of vacuum polarization, where m_e and e are the electron mass and charge, respectively.

BH mass $10M_\odot$ and effective charge to mass ratio of ~ 0.1

$$N_{e^+e^-} = 2 \times 10^{58}$$

$$\tau \sim \sigma_T \bar{n}_{e^+e^-} \times [r_2 - r_1] \sim 10^{16} - 10^{21} \gg 1$$

- $e^+ e^-$ plasma-Baryon expansion because of its internal pressure!

MeV radiation

Ultrarelativistic velocity $\Gamma \sim 100$

Kerr BH+B0

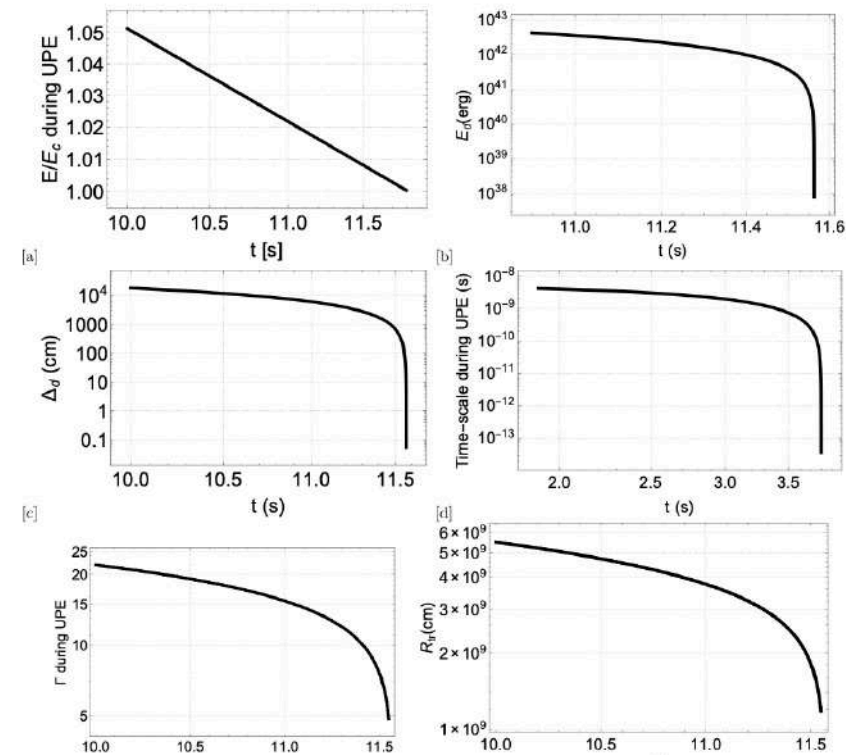
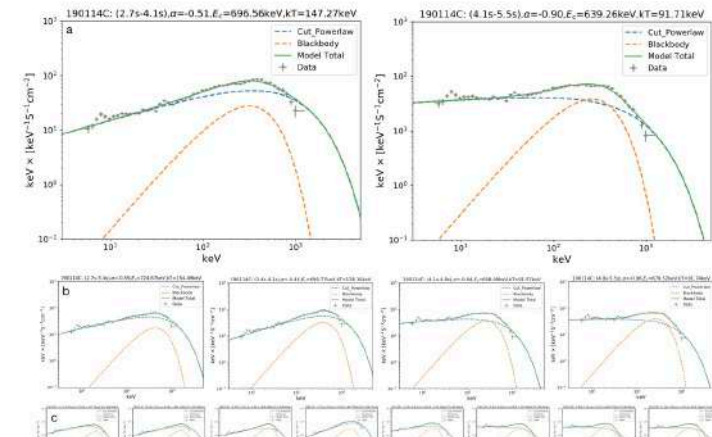
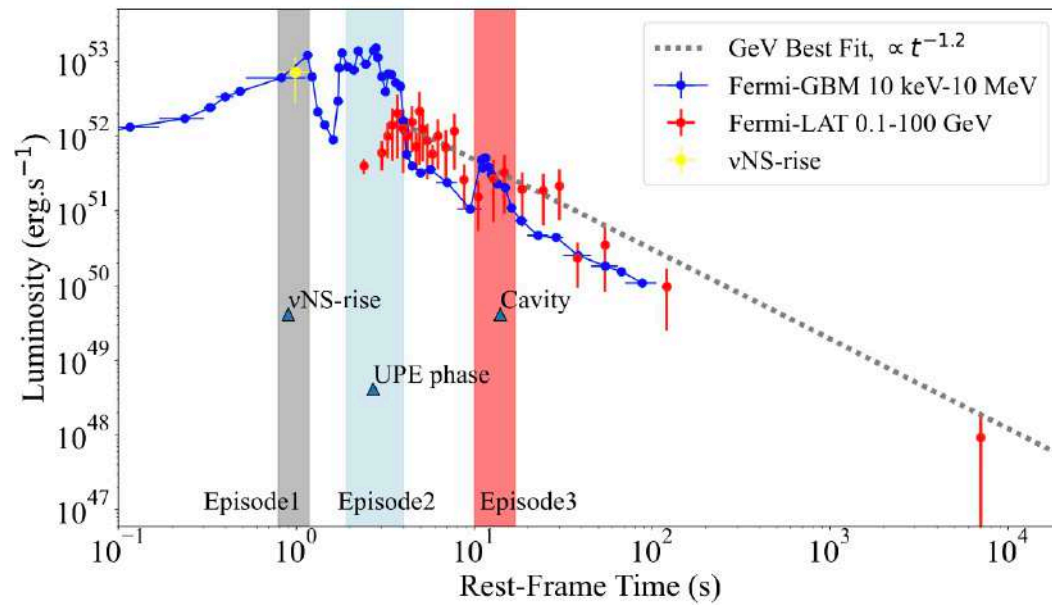
$E > E_c$

Baryon load

Damour and Ruffini, PRL, 463 (1975)
 Ruffini, Salmonson, Wilson, and Xue, A&A 350, 334 (1999)
 Ruffini, Salmonson, Wilson, and Xue, A&A 359, 855 (2000)

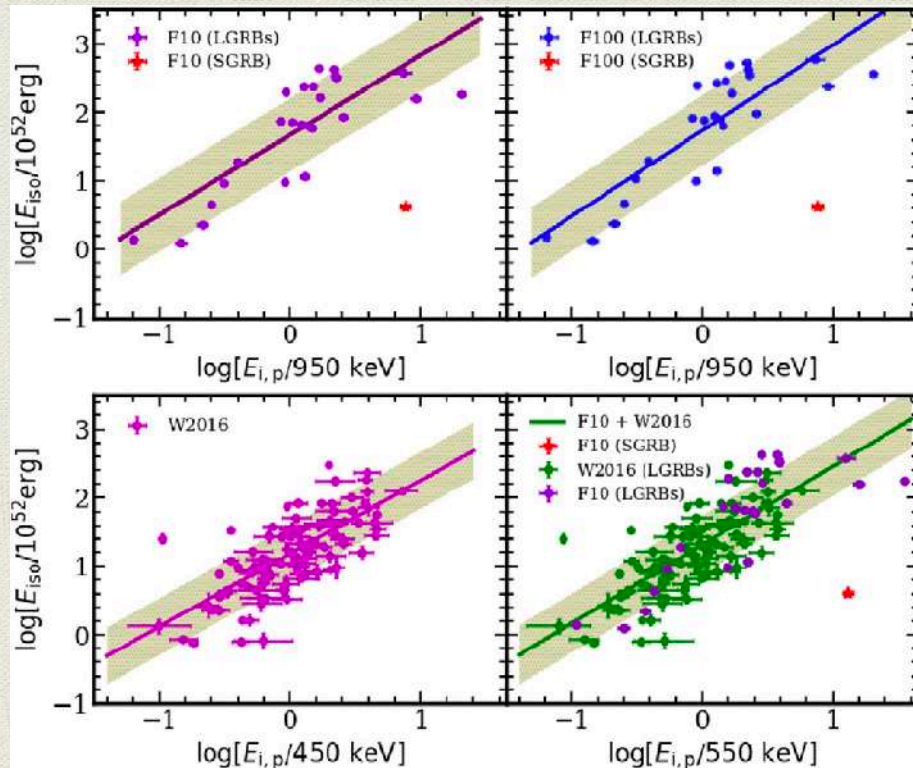
GRB 190114C: Ultra Relativistic Prompt Emission Phase (UPE)

Moradi, Rueda, Ruffini, Li, et al., PRD 104, 063043 (2021).



Phenomenological Relation

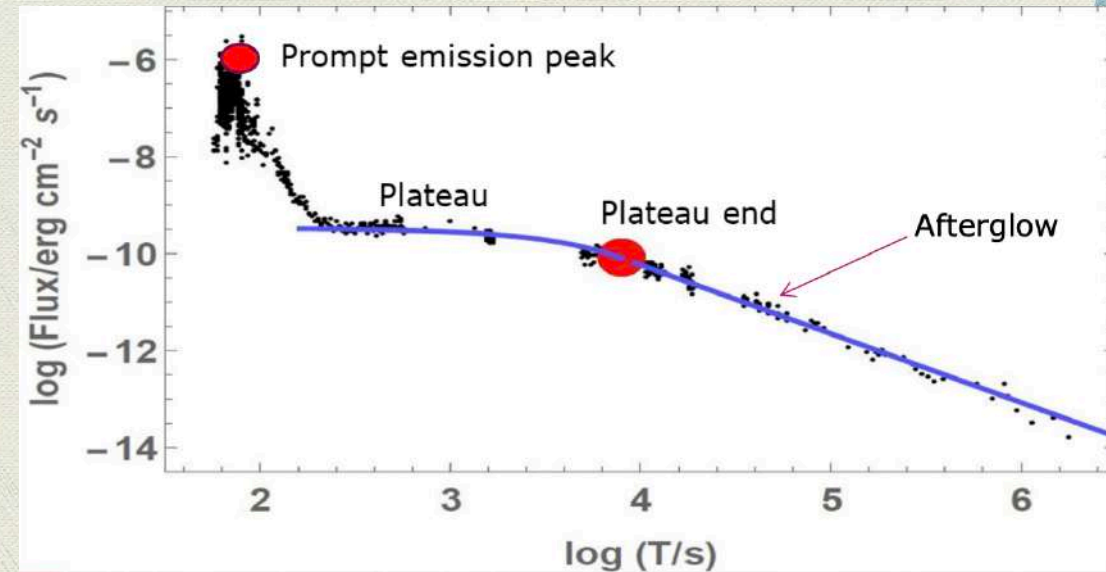
Amati Relation



$$E_{p,i} = K \times (E_{iso}/10^{52} \text{ erg})^m$$

Dainotti et al., MNRAS 2008

$$\log L_X = \log a + b \log T_a$$



Highly Magnetized NSs (Magnetar) in GRBs: Dipolar Component

- Short and long GRBs

- Explains afterglow

Highly magnetized NS is formed after WD-RD / WD merger

This magnetic field produces an Electric Field

Overcritical E field produces electron positron pair plasma

$$E \rightarrow e^+ + e^- + E$$

$$\gamma + B \rightarrow e^+ + e^- + B$$

Plasma expands and in radius around 10^9 - 10^{14} cm it starts to radiate

nature

Explore content

About the journal

Publish with us

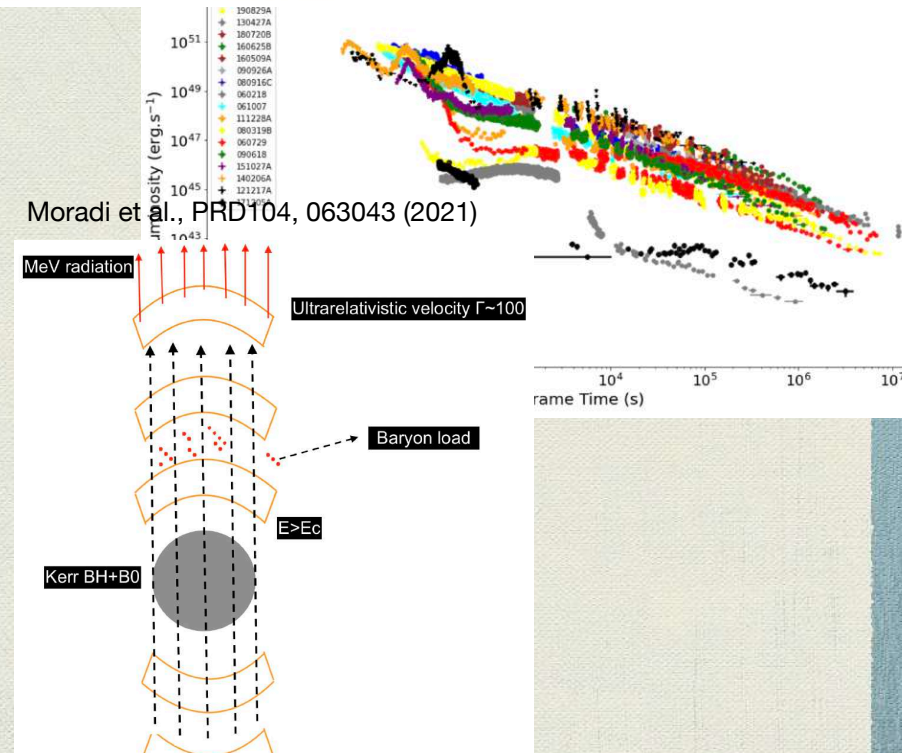
nature > letters > article

Letter | Published: 11 June 1992

Millisecond pulsars with extremely strong magnetic fields as a cosmological source of γ -ray bursts

V. V. Usov

Nature 357, 472–474 (1992) | Cite this article



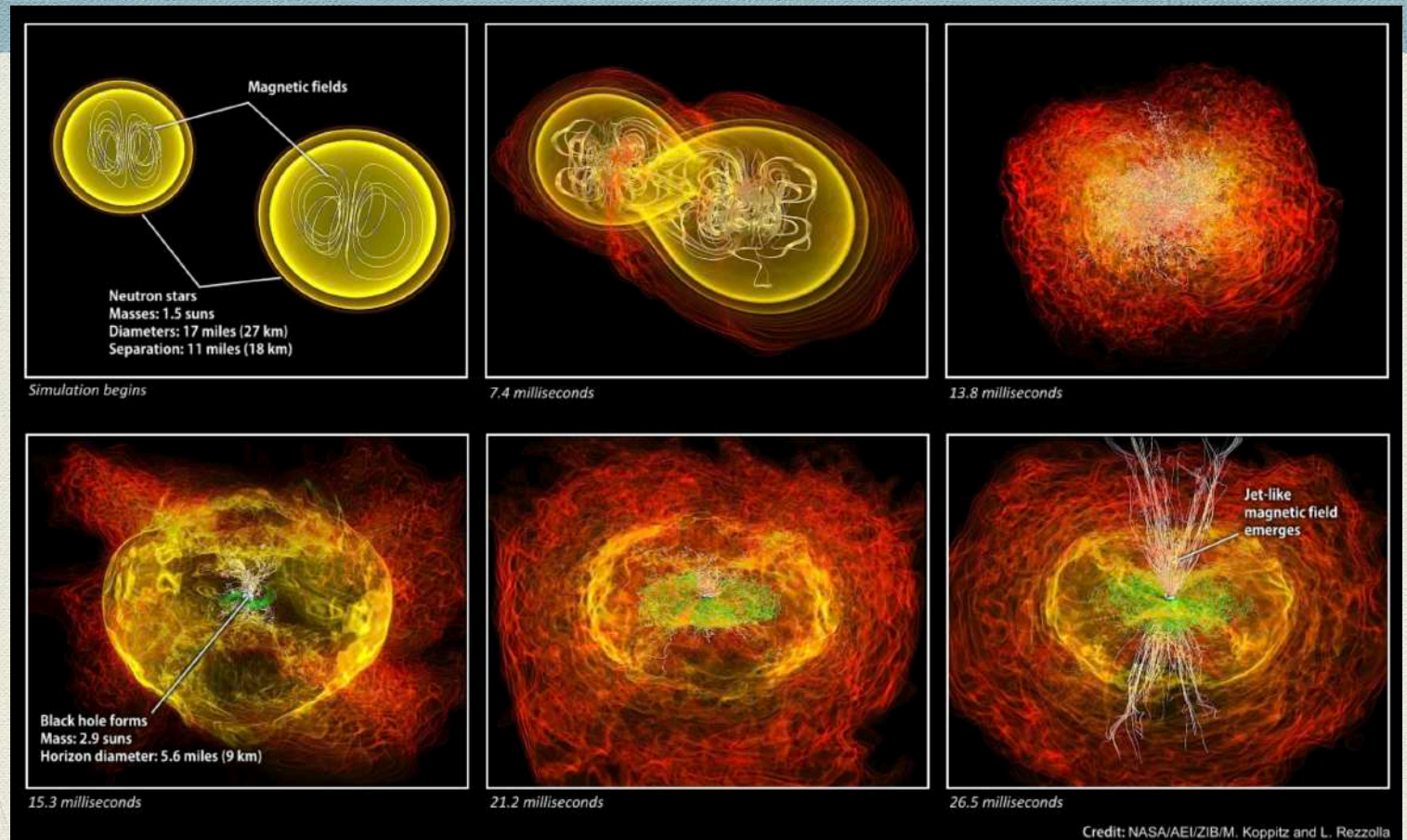
Similar idea for BH pulsar

◆ Short GRBs (NS-NS mergers): Afterglow

◆ **supra-massive NS**

◆ Stable NS

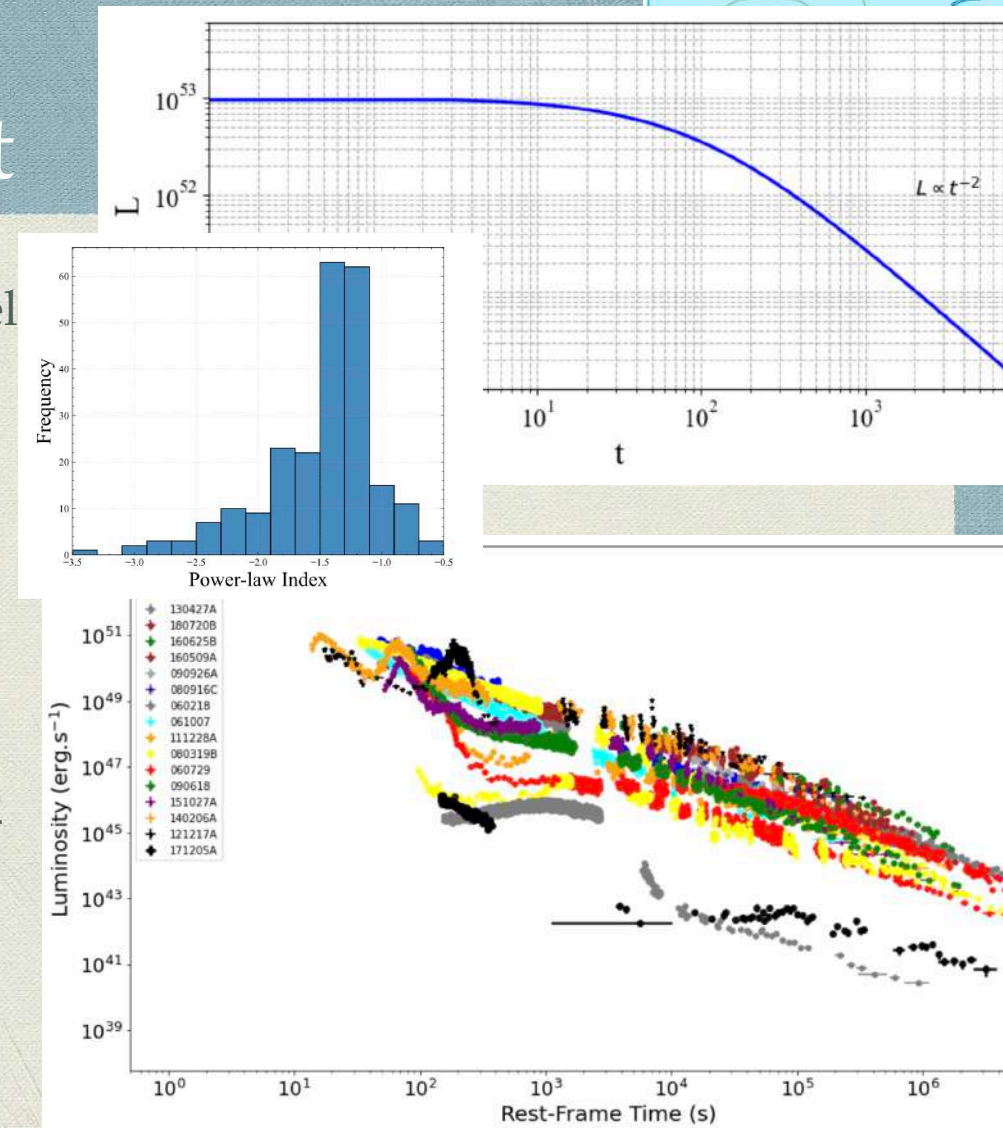
◆ BH



• **The role of supra-massive NS is more pronounced**

Gamma-ray bursts (GRBs): Dipolar Component

- ◆ Our understanding of the Magnetic field: Dipolar field
- ◆ Afterglow of GRBs: Newborn highly magnetized Neutron stars or Magnetars
- ◆ Dipole component has limits in explaining the afterglow;
- ◆ Although it was successful in some aspects, but t^{-2} cannot explain majority of the afterglows
- ◆ Observation: $t^{-\alpha}$; $\alpha = 1.48 \pm 0.32$



Multipolar Expansion

$$\frac{dE_{\text{rot}}}{dt} = I\Omega\dot{\Omega} = -L$$

Wang, Moradi, Li, The Astrophysical Journal, 974:89 (2024)

Dipole

$$\Omega = \Omega_0 \left(1 + \frac{t}{\tau_{\text{dip}}}\right)^{-1/2},$$

$$L_{\text{dip}} = L_{\text{dip},0} \left(1 + \frac{t}{\tau_{\text{dip}}}\right)^{-2}$$

$$\tau_{\text{dip}} = \frac{3Ic^3}{4\Omega_0^2 B_{\text{dip}}^2 R^6 \Theta_{\text{dip}}^2}$$

$$L_{\text{dip},0} = \frac{I\Omega_0^2}{2\tau_{\text{dip}}}$$

Quadrupole

$$\Omega = \Omega_0 \left(1 + \frac{t}{\tau_{\text{quad}}}\right)^{-1/4},$$

$$L_{\text{quad},0} = \frac{I\Omega_0^2}{4\tau_{\text{quad}}}$$

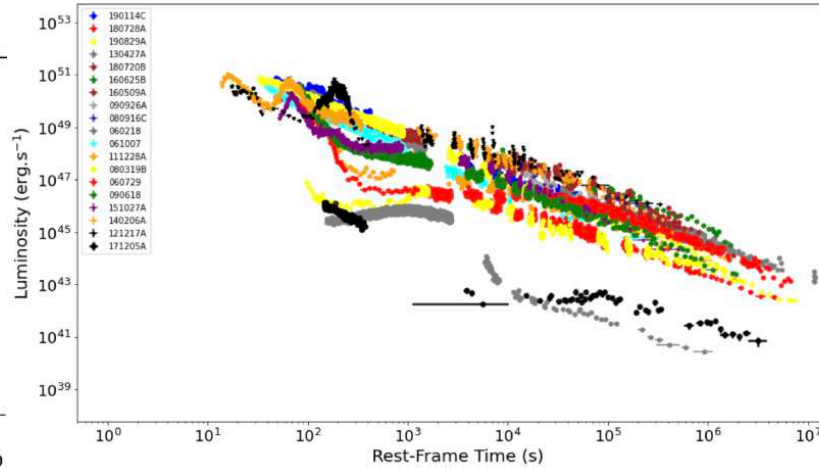
Hexapole

$$\Omega = \Omega_0 \left(1 + \frac{t}{\tau_{\text{hexa}}}\right)^{-1/6},$$

$$L_{\text{hexa}} = L_{\text{hexa},0} \left(1 + \frac{t}{\tau_{\text{hexa}}}\right)^{-4/3}$$

$$\tau_{\text{hexa}} = \frac{4725\pi I c^7}{12\Omega_0^6 B_{\text{hexa}}^2 R^{10} \Theta_{\text{hexa}}^2}$$

$$L_{\text{hexa},0} = \frac{I\Omega_0^2}{6\tau_{\text{hexa}}}$$

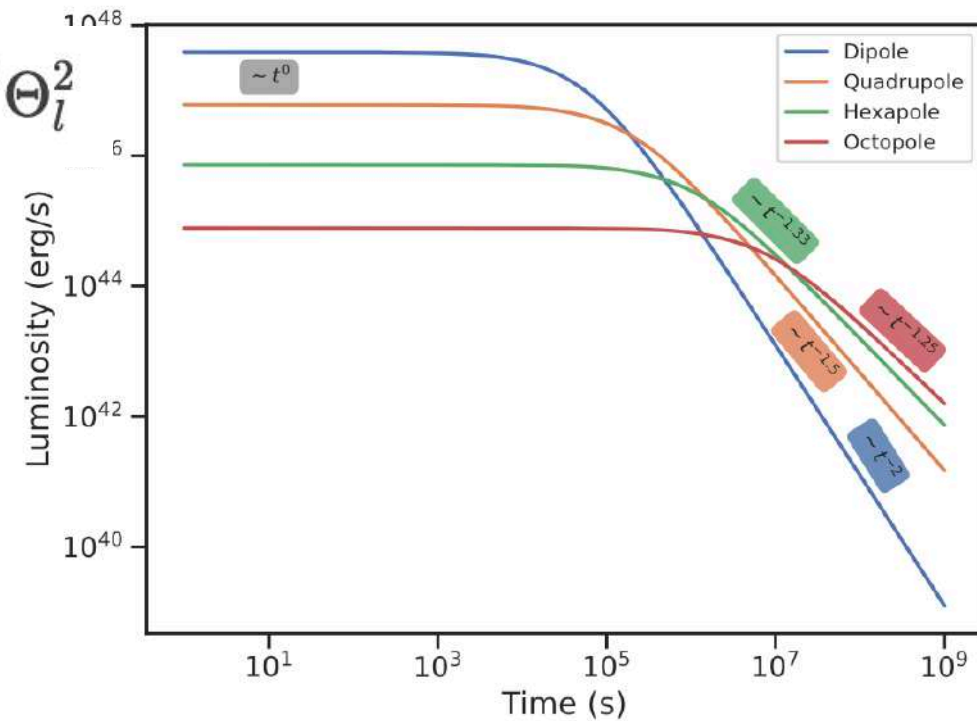


Multipolar Spin-Down of Newborn Magnetars

- Higher-order multipoles (quadrupole, hexapole, octopole) dominate spin-down in newborn millisecond magnetars.

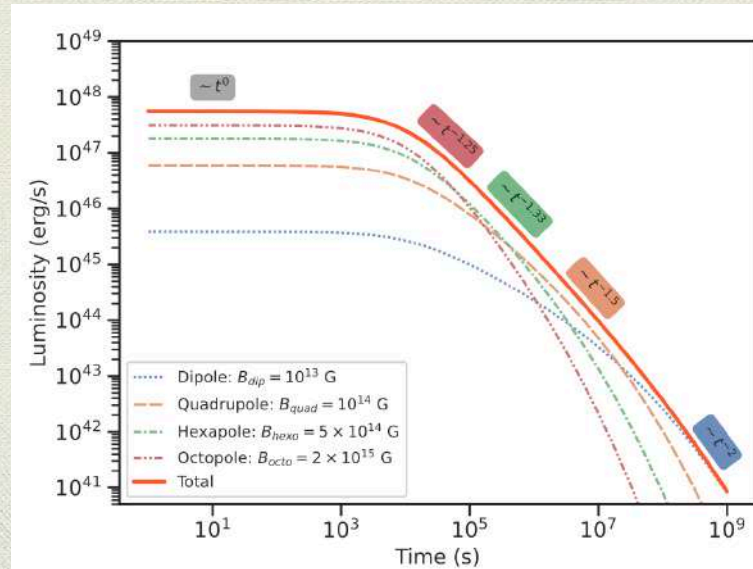
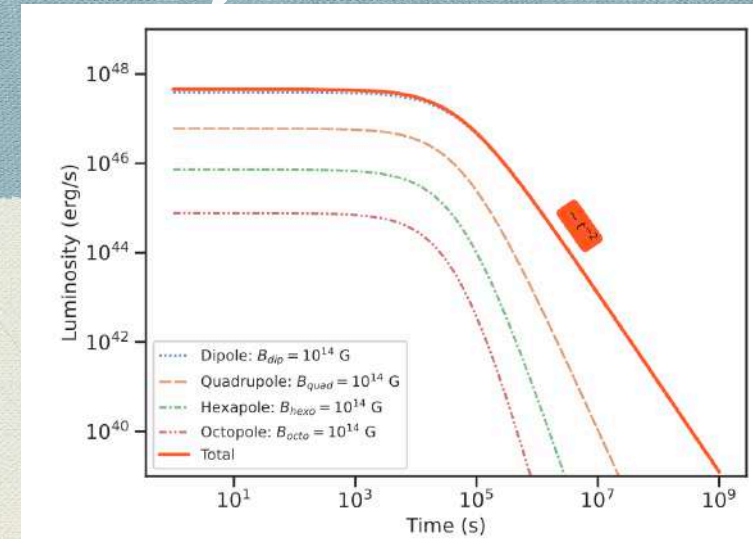
- Spin-down luminosity: $L_l = C_l \Omega^{2l+2} B_l^2 R^{2l+4} \Theta_l^2$

- Dipole ($l=1$): $L \propto \Omega^4 \rightarrow$ decay index -2
- Quadrupole ($l=2$): $L \propto \Omega^6 \rightarrow$ decay index -1.5
- Hexapole ($l=3$): $L \propto \Omega^8 \rightarrow$ decay index -1.33
- Example: SGR 0418+5729 shows weak dipole but strong multipoles ($\sim 10^{15}$ G).
- Figure: Luminosity vs. time for single multipoles



Magnetic Field Scenarios & Luminosity Evolution

- Fig 1: All multipoles, same $B \rightarrow$ dipole dominates at all times.
- Fig 3: Increasing B with l :
 - Early: High- l (e.g., octopole) dominates
 - After $\sim 10^8$ s (~ 3 yr): Dipole takes over
- Multipoles exceed dipole luminosity in early phases



Solving the GRB Afterglow Puzzle

- Swift-XRT: 204 GRBs with plateaus → decay slopes peak at -1.55 (range -1 to -2).
- Matches multipolar predictions (quad: -1.5, hex: -1.33).
- Reduced χ^2 ; better fit, F-test for the nested models.
- $L_{\text{bol}} \approx 5 \times L_{\text{XRT}}$

$$L_{\text{tot}}(t) = \sum_{l=1}^{\infty} L_l(t). \quad (2)$$

Since the rotational energy loss satisfies

$$\dot{E}_{\text{rot}} = I \Omega \dot{\Omega} = -L_{\text{tot}}(t) \quad (3)$$

one immediately gets

$$I \Omega \dot{\Omega} = - \sum_{l=1}^{\infty} C_l B_l^2 R^{2l+4} \Theta_l^2 \Omega^{2l+2} \implies$$

$$\dot{\Omega} = - \sum_{l=1}^{\infty} K_l \Omega^{2l+1},$$

with $K_l = C_l B_l^2 R^{2l+4} \Theta_l^2 / I$. We treat it as a separable ordinary differential equation:

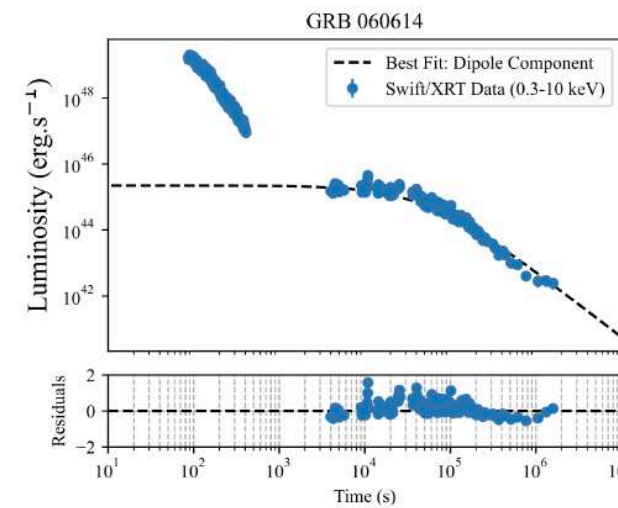
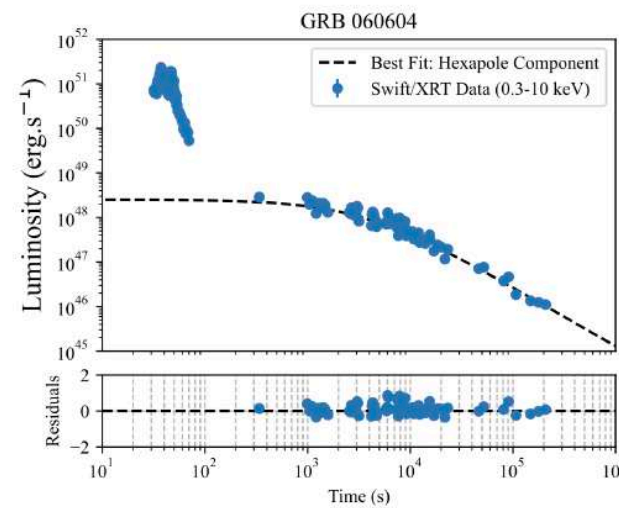
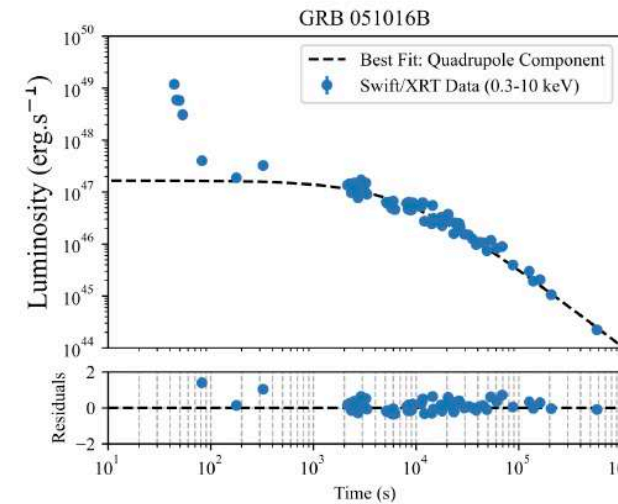
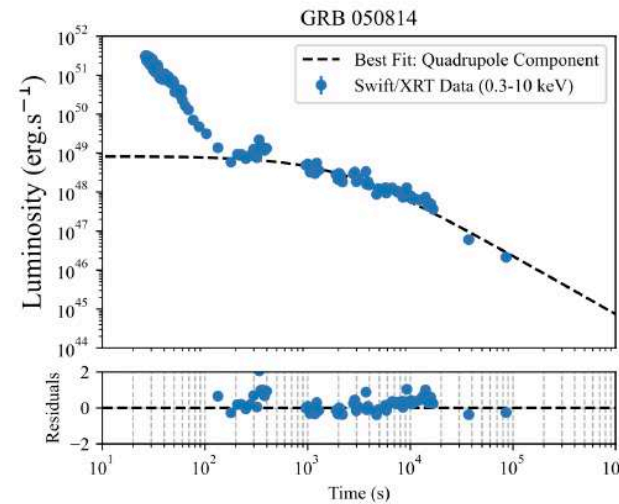
$$\frac{d\Omega}{\sum_{l=1}^{\infty} K_l \Omega^{2l+1}} = -dt,$$

$$\int_{\Omega_0}^{\Omega(t)} \frac{d\Omega'}{\sum_{l=1}^{\infty} K_l \Omega'^{2l+1}} = - \int_{t_0}^t dt' = -(t - t_0).$$

This integral is the *implicit* solution:

$$t = t_0 + \int_{\Omega(t)}^{\Omega_0} \frac{d\Omega'}{\sum_{l=1}^{\infty} K_l \Omega'^{2l+1}}. \quad (4)$$

- 4 GRBs fitted with multipolar spin-down:
- GRB 050814/051016B: Quadrupole-dominated
- GRB 060604: Hexapole-dominated
- GRB 060614: Dipole-dominated



Evidence for Multipolar Fields in Various Neutron Stars

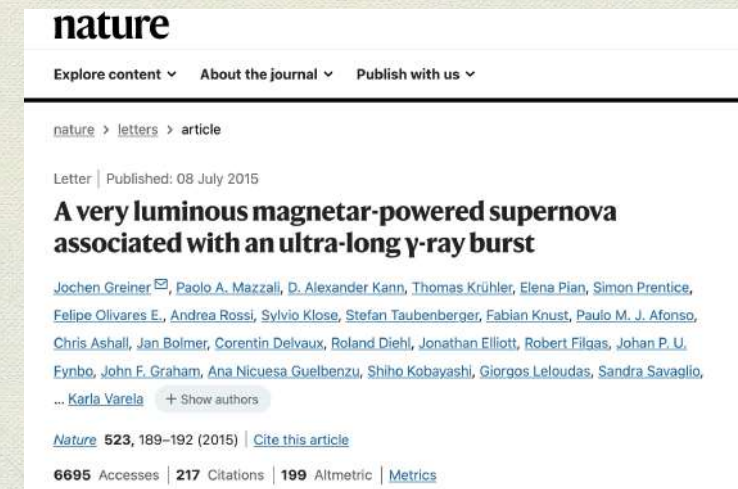
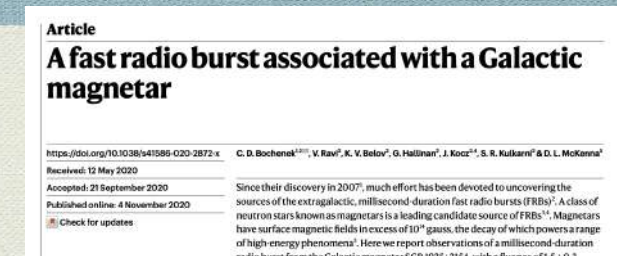
- Multipolar fields are essential for pair production in NS magnetospheres.
- Observational and simulation advances demand multipolar components.
- SGR 0418+5729:
 - Dipole $B \sim 10^{12}$ G (spin-down)
 - Multipole $B \sim 10^{15}$ G (cyclotron lines)
- PSR J0030+0451 (NICER): Thermal X-ray pulsations imply multipoles.
- Required to explain flares, irregular timing, and detailed X-ray features.
- Younger magnetars (e.g., SGR J1935+2154, SGR 0418+5729) show strong multipoles:
 - $B_{\text{dip}} \sim 4 \times 10^{14}$ G, $B_{\text{non-dip}} \sim 10^{15}$ G
- Aged magnetars \rightarrow dominant dipoles; younger ones \rightarrow pronounced multipoles.
- Early-stage data scarce: CDF-S XT2 is the only known young magnetar (post NS merger).



NASA's NICER Tracks a Magnetar's Hot Spots -
NASA SVS

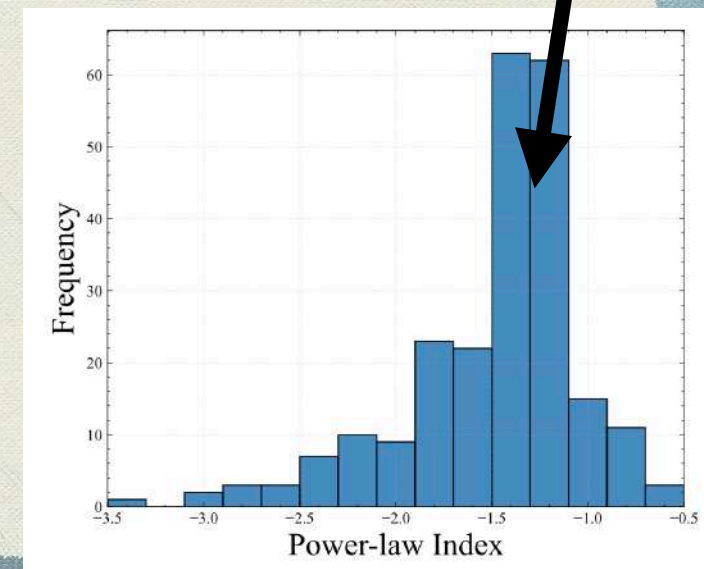
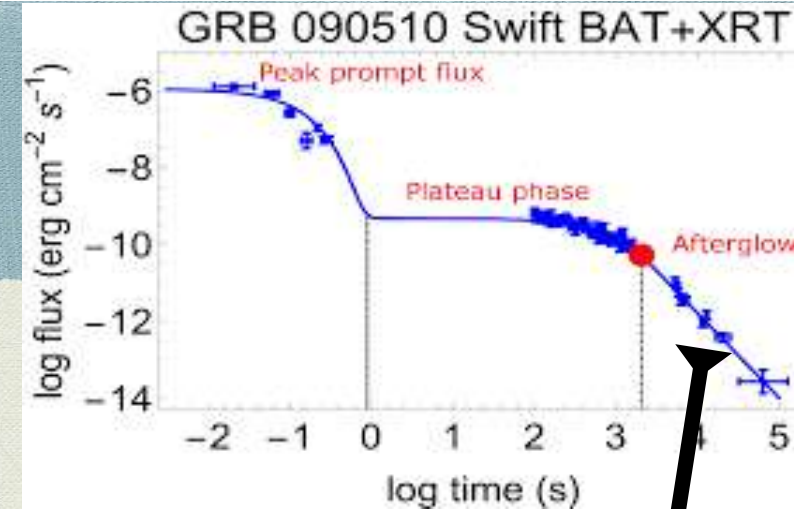
Possible Newborn Magnetars

- ❖ The formation of magnetar is associated with and plays a critical role in various areas of astrophysics;
- ❖ Superluminous supernova (SLSNs);
- ❖ **Gamma-ray bursts (GRBs);**
- ❖ Fast radio bursts (FRBs);



Dainotti Relation & Magnetar Model

- Dainotti Relation: $\log L_x = \log a + b \log T_{a*}$ ($b \approx -1.07$)
- Purpose: Standardizes GRBs, probes central engine physics.
- Central Engine: Magnetars (highly magnetized neutron stars).
- Issue: Dipole spin-down predicts $\alpha = -2$.
- Observation: Swift-XRT data (238 GRBs) show α in $[-1, -2]$.
- Figure: Distribution of decay indices α (79% between -1 and -2, median -1.39).



Multipolar Spin-Down Model

- Magnetars may have higher-order multipoles ($l = 2, 3 \dots$).

$$L_l = C_l \Omega^{2l+2} B_l^2 R^{2l+4} \Theta_l^2$$

- Luminosity:

- Decay index $\alpha = -(1 + 1/l)$

- Higher l : stronger early emission, steeper early decay.

- Figure: Spin-down luminosity vs time for various multipoles

In Practice: Single multipole is dominant **Dainotti et al., MNRAS 2008**
Single multipole

$$L_{l,0} = \frac{I \Omega_0^2}{2l \tau_l},$$

$$L_{l,0} \propto \tau_l^{-1}.$$



$$\log L_X = \log a + b \log T_a$$

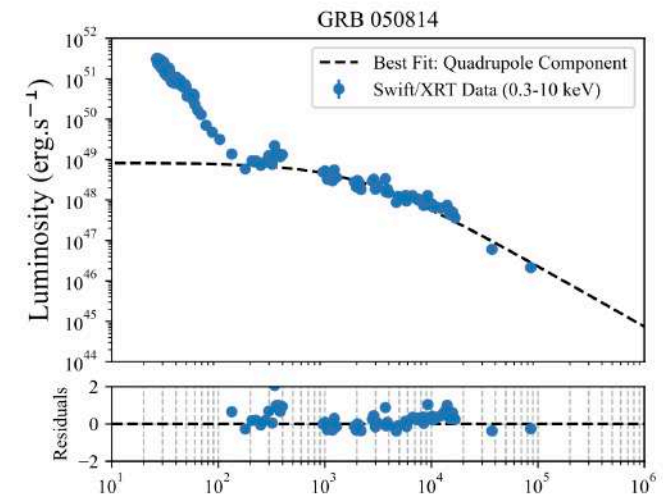
$$b = -1.07^{+0.09}_{-0.14}$$

$$\Omega = \Omega_0 \left(1 + \frac{t}{\tau_l}\right)^{-2l},$$

$$L = L_{l,0} \left(1 + \frac{t}{\tau_l}\right)^{-1-1/l}.$$

$$\tau_l = \frac{I C^{2l+1}}{(2l+2) C_l \Omega_0^{2l} B_l^2 R^{2l+4} \Theta_l^2}$$

$$L_{l,0} = \frac{I \Omega_0^2}{2l \tau_l}$$



Explaining the Dainotti Relation

$$M = 1.4 M_{\odot}$$

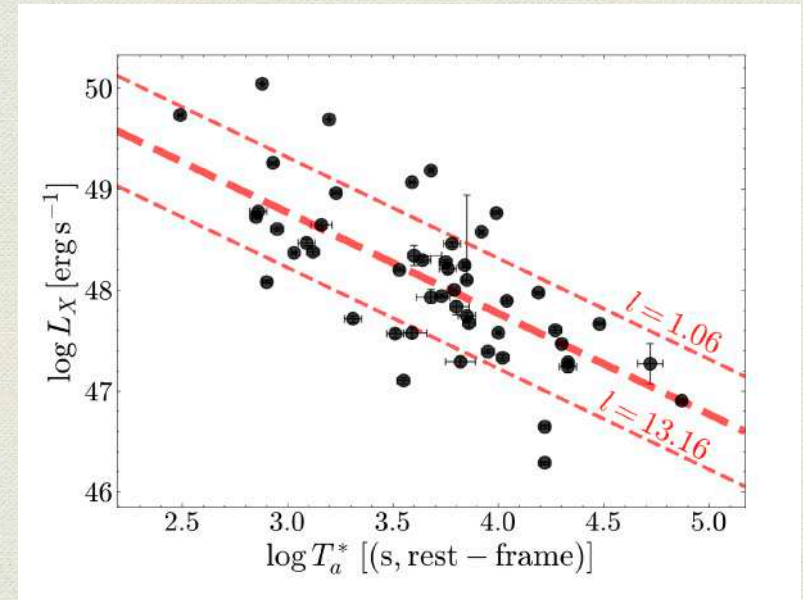
$$L_{l,0} = \frac{I\Omega_0^2}{2l\tau_l}$$



$$L_{l,0}^{UL} = \frac{2.2 \times 10^{52}}{l \tau_l}$$

$$R = 10 \text{ km, and } P_0 = 1 \text{ ms}$$

- Multipolar spin-down gives $b \approx -1$ slope: $\log L_X \propto -\log T_{a*}$
- Normalization varies with “ l ”
- Observed upper limit for Platinum GRBs sample imply $l \sim 1.06$ for the upper limit.



Caveats and Limitations

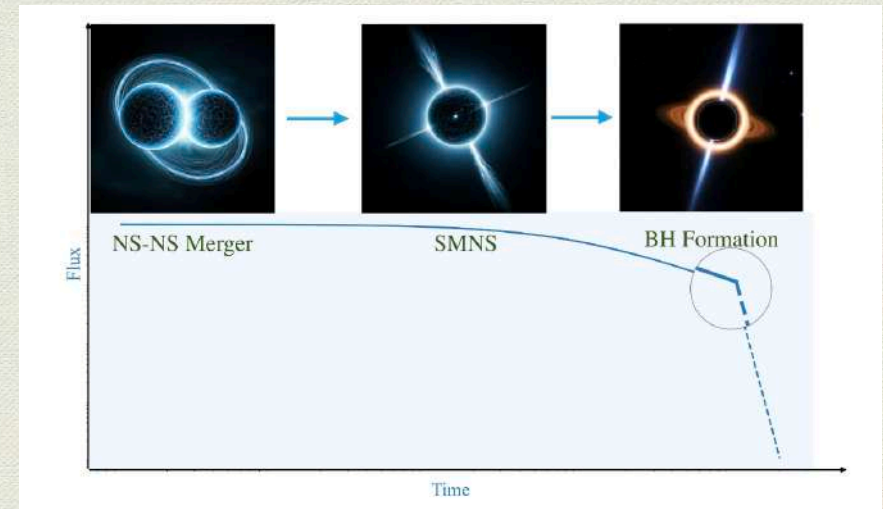
1. Plateau emission may arise from external shocks.
2. Jet geometry and efficiency affect true luminosity.
3. Plasma/Wind effects.
4. Black hole models (e.g., Blandford–Znajek) can mimic relation.

Conclusions and Future Work

- Multipolar model explains slope and decay index range.
- Higher-order multipoles dominate early emission.
- Future work:
 - - Constrain \mathcal{E}_x and θ_j for individual GRBs.
 - - Use multiwavelength data to refine estimates.
 - - Explore hybrid central engine models.
- Implication: Magnetars with multipoles can unify GRB afterglow behavior.

Probing Neutron Star EOS via SGRB Magnetar Collapse

- SGRB “internal plateaus” suggest supramassive magnetars temporarily stable via rapid rotation.
- Collapse time (t_{co}) and X-ray decay constrain mass–spin conditions at BH formation.
- Goal: Probe the Equation of State (EOS) of neutron stars at supranuclear densities.
- Why It Matters: EOS determines maximum mass (M_{TOV}), radii, and phase transitions (e.g., quark matter).
- Figure: NS merger \rightarrow SMNS \rightarrow X-ray plateau \rightarrow BH collapse

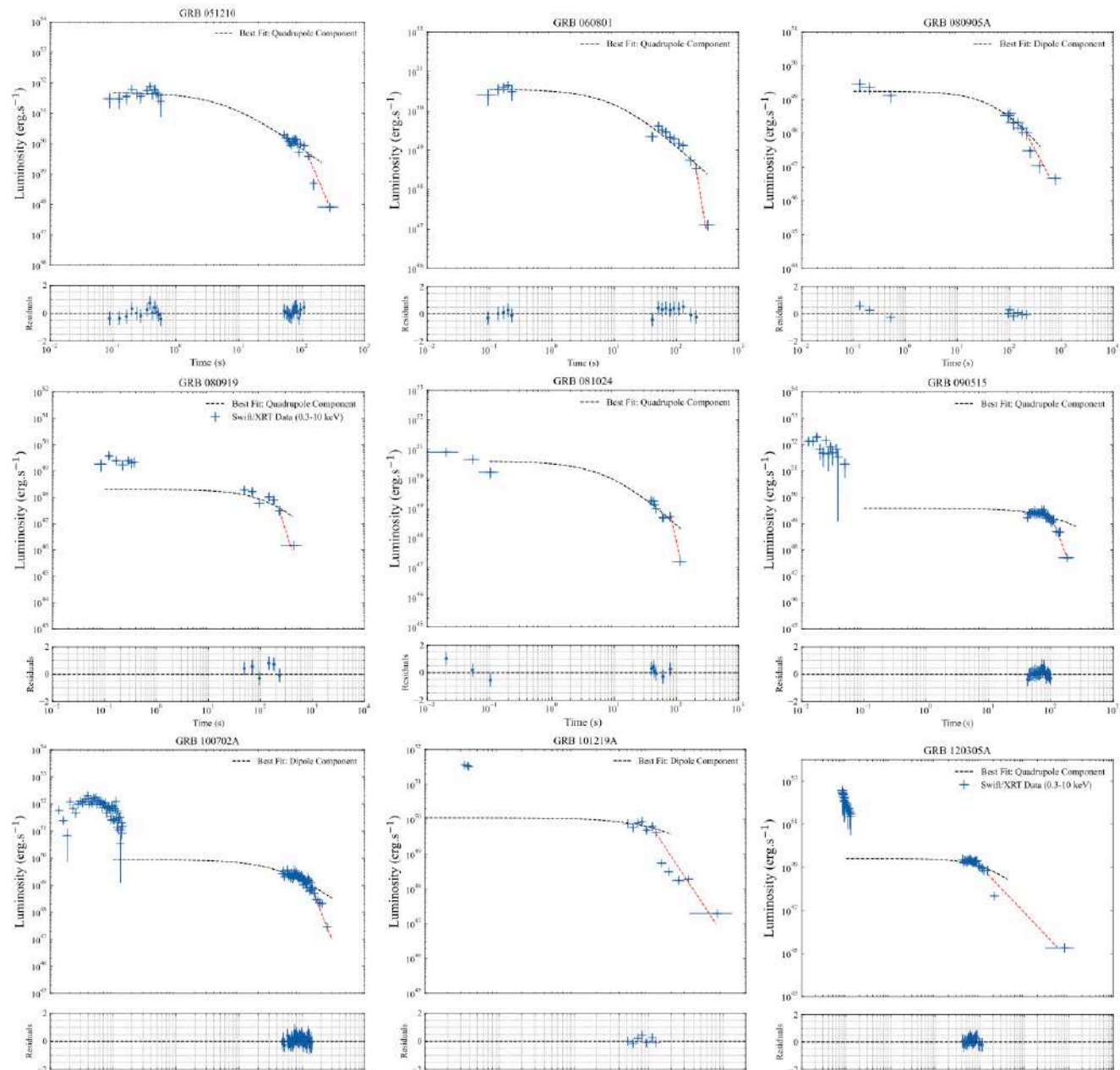


schematic

Modeling SGRB Plateaus with Multipolar Magnetic Fields

SGRB	z	E_{iso} (erg)	P_0 (ms)	B_{dip} (10^{15} G)	B_{quad} (10^{15} G)	Collapse time (s)	E_{PD} (erg)	ΔP (ms)
051210	(0.72)	$5.98^{+13.5}_{-4.05} \times 10^{51}$	1.01 ± 0.29	—	13.7 ± 0.9	120 ± 13	$(1.68 \pm 0.44) \times 10^{51}$	3.2 ± 0.1
060801	1.13	$1.17^{+1.79}_{-0.71} \times 10^{53}$	2.7 ± 0.1	—	69.8 ± 0.9	220 ± 24	$(2.68 \pm 0.74) \times 10^{50}$	6.4 ± 0.5
080905A	0.122	$6.16^{+12.3}_{-4.03} \times 10^{50}$	6.9 ± 0.3	18.7 ± 0.2	—	214 ± 12	$(6.1 \pm 0.41) \times 10^{49}$	22.6 ± 0.6
080919	(0.72)	$5.18^{+9.34}_{-3.26} \times 10^{51}$	15.1 ± 0.3	21.6 ± 1.1	—	233 ± 35	$(3.91 \pm 1.01) \times 10^{49}$	21 ± 3
081024	(0.72)	$5.65^{+7.53}_{-3.16} \times 10^{51}$	5.2 ± 0.4	32.5 ± 0.4	—	80 ± 10	$(1.5 \pm 0.24) \times 10^{50}$	10 ± 0.6
090515	(0.72)	$3.44^{+3.55}_{-1.55} \times 10^{50}$	2.8 ± 0.1	3.6 ± 0.3	—	100 ± 3	$(3.8 \pm 0.81) \times 10^{50}$	11 ± 0.1
100702A	(0.72)	$2.28^{+1.46}_{-0.80} \times 10^{51}$	2.9 ± 0.1	6.8 ± 0.7	—	148 ± 2	$(1.72 \pm 0.37) \times 10^{50}$	16 ± 0.1
101219A	0.718	$1.69^{+0.79}_{-0.54} \times 10^{53}$	1.6 ± 0.4	1.9 ± 0.9	—	125 ± 13	$(2.59 \pm 0.28) \times 10^{51}$	3.4 ± 0.2
120305A	(0.72)	$2.02^{+0.10}_{-0.10} \times 10^{52}$	3.7 ± 0.1	6.4 ± 0.8	—	150 ± 27	$(6.17 \pm 1.2) \times 10^{50}$	6.7 ± 0.1
120521A	(0.72)	$8.42^{+12.19}_{-4.95} \times 10^{51}$	9.2 ± 0.3	11.4 ± 0.5	—	144 ± 40	$(1.36 \pm 0.39) \times 10^{50}$	12.1 ± 0.4

- Data Source: 10 SGRBs with Swift-BAT/XRT internal plateaus + rapid decay (Table).
- Spin-down Luminosity: $L_l(t) \propto B_l^2 \Omega^{2l+2}(t)$
- Multipolar spin-down (quadrupole, hexapole) better fits than dipole.
- Fitting: LMFIT used; F-tests confirm higher-order field components (e.g., GRB 051210).
- Collapse Time (t_{co}): Sharp luminosity drop \rightarrow exceeds $M_{\text{crit}}(\alpha)$.



From Magnetar Collapse to Kerr Black Hole Spin Extraction

Christodoulou (1970); Christodoulou & Ruffini (1971); Hawking (1971):

BH

EOS	$M_{\text{crit}}^{J=0}$ (M_{\odot})	k	l	R (km)	I (10^{45} g cm^2)
TM1	2.20	0.017	1.61	12.5	2.81
GM1	2.39	0.011	1.69	12.1	3.12
NL3	2.81	0.006	1.68	13.8	4.99

NS

$$M_{\text{crit}}(j) = M_{\text{crit}}^{J=0}(1 + kj^p),$$

Cipolletta et al. (2015)

The energy condition is obtained from the mass-energy formula of the Kerr BH [1–3]

$$M^2 = \frac{c^2 J^2}{4G^2 M_{\text{irr}}^2} + M_{\text{irr}}^2. \quad (1)$$

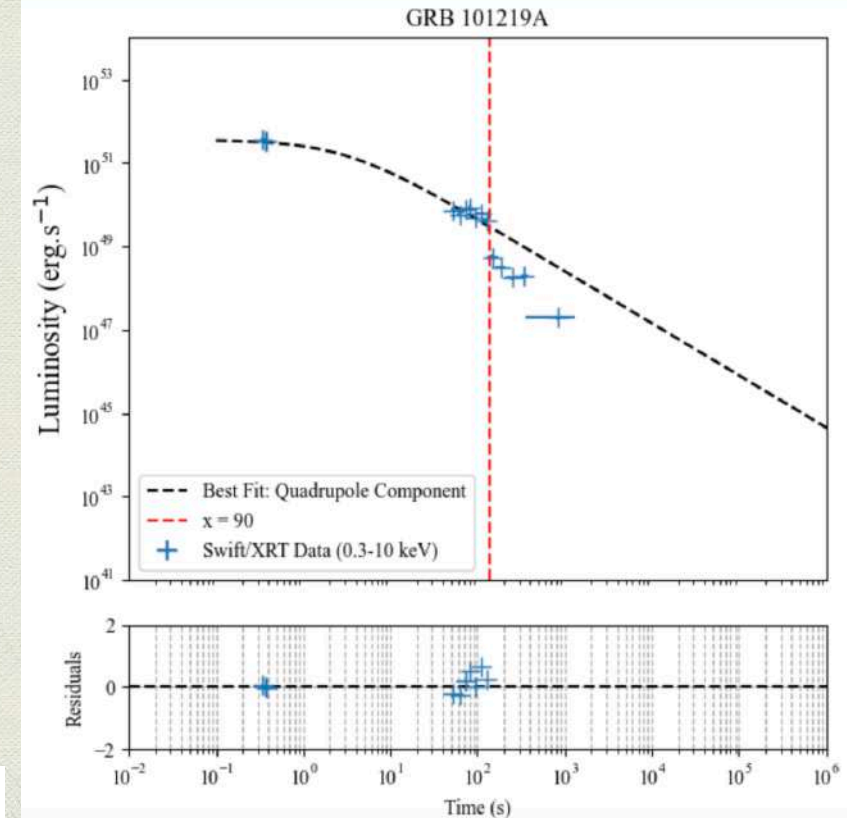
The extractable energy of a Kerr BH E_{ext} is given by the subtracting the irreducible mass, M_{irr} , from the total mass of the BH, M :

$$E_{\text{ext}} = (M - M_{\text{irr}})c^2 = \left(1 - \sqrt{\frac{1 + \sqrt{1 - \alpha^2}}{2}}\right) Mc^2. \quad (2)$$

which we use to obtain M as a function of α , $M(\alpha)$, by requesting the condition that observed post-plateau (PP) emission originates from BH extractable energy, i.e.

$$E_{\text{PP}} = E_{\text{ext}}. \quad (3)$$

BH's MASS \geq NS's MASS $M \geq M_{\text{crit}}(\alpha) = M_{\text{TOV}}(1 + kj^l)$



From Magnetar Collapse to Kerr Black Hole Spin Extraction

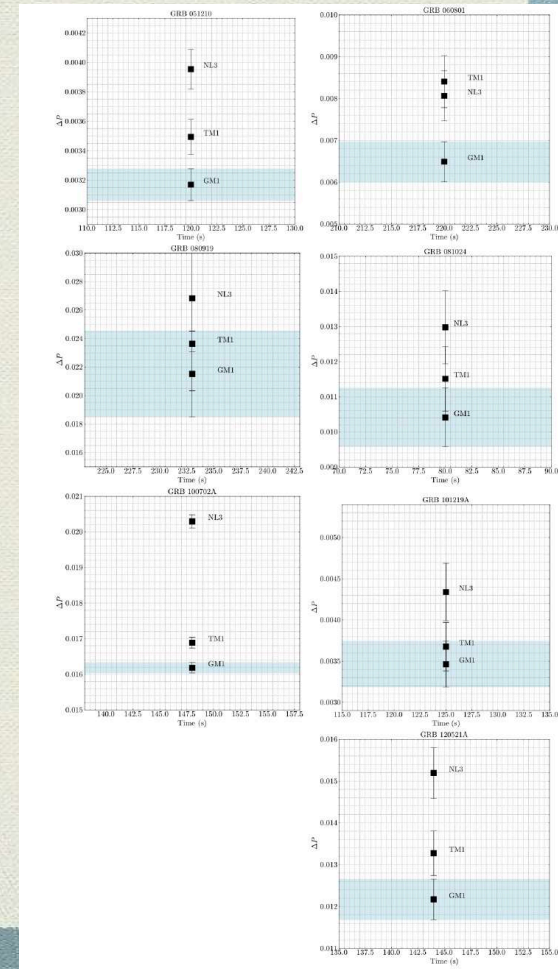
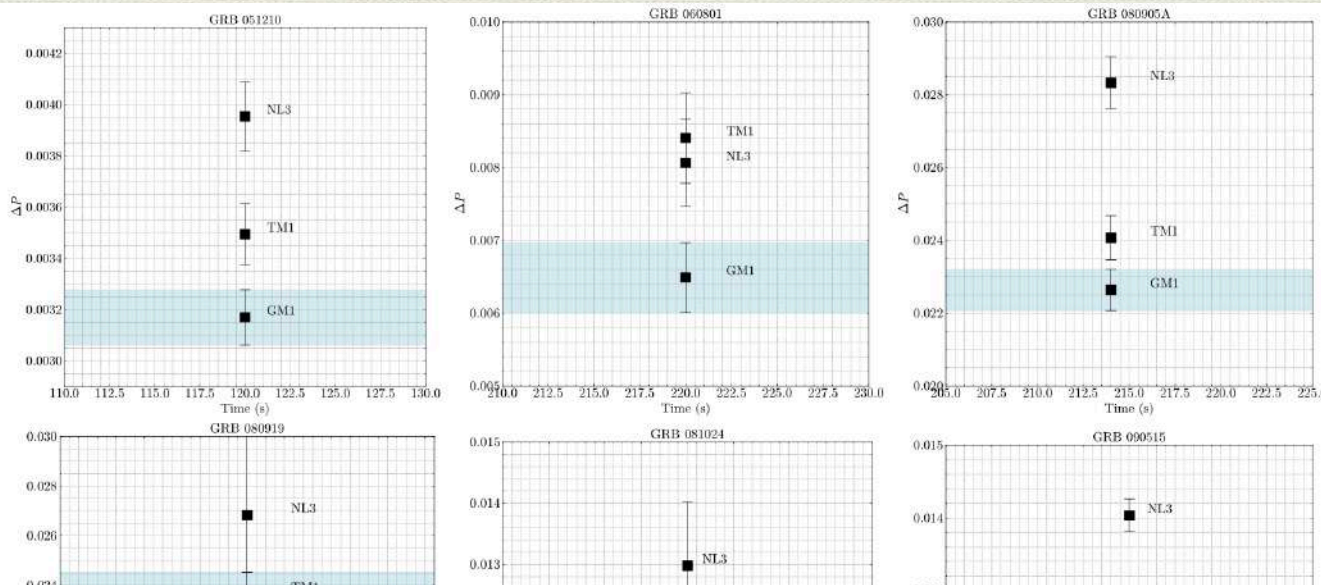
EOS	$M_{\text{crit}}^{J=0}$ (M_{\odot})	k	l	R (km)	I (10^{45}g cm^2)
TM1	2.20	0.017	1.61	12.5	2.81
GM1	2.39	0.011	1.69	12.1	3.12
NL3	2.81	0.006	1.68	13.8	4.99

- Collapse Criterion: $M \geq M_{\text{crit}}(\alpha) = M_{\text{TOV}}(1 + k j^l)$ EOS-dependent (Table).
- Post-collapse Energy:

$$E_{\text{ext}} = \left(1 - \sqrt{\frac{1 + \sqrt{1 - \alpha^2}}{2}} \right) M c^2$$
- Powered by Blandford-Znajek process? We don't care at this stage.
- Observational Match: Integrated X-ray tail luminosity E_{PD} constrains M, α at collapse.

EOS Selection via Spin Period Matching

- Strategy: Compare P_{NS} (from spin-down) to P_{BH} (from Kerr energy at t_{co}).
- Best EOS Fit: GM1 ($M_{\text{TOV}} = 2.39 \text{ Msun}$) minimizes $\Delta P = |P_{\text{NS}} - P_{\text{BH}}|$.
- Disfavored EOSs: TM1 (soft), NL3 (stiff).
- Figure: ΔP distribution



Model Assumptions and Limitations

• Assumptions:

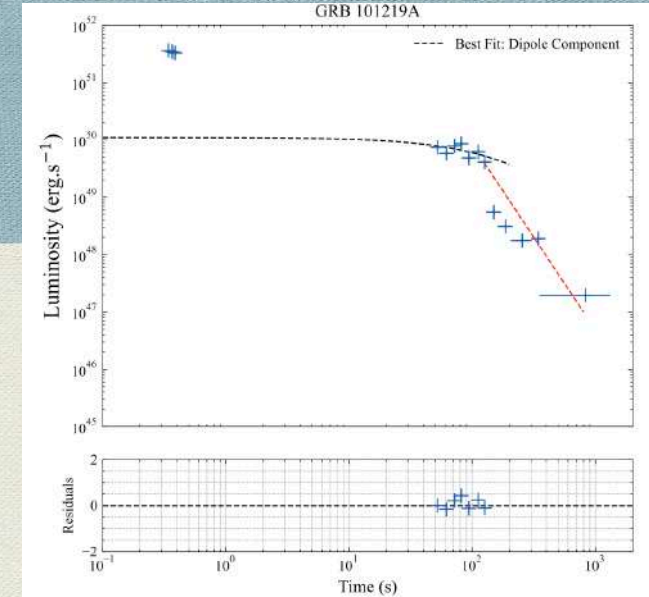
- 1. Plateaus powered by magnetar (wind), not external shocks.
- 2. Constant radiative efficiency and jet angle.
- 3. Full Kerr energy extraction (no GW/accretion losses/radiation efficiency).

• Limitations:

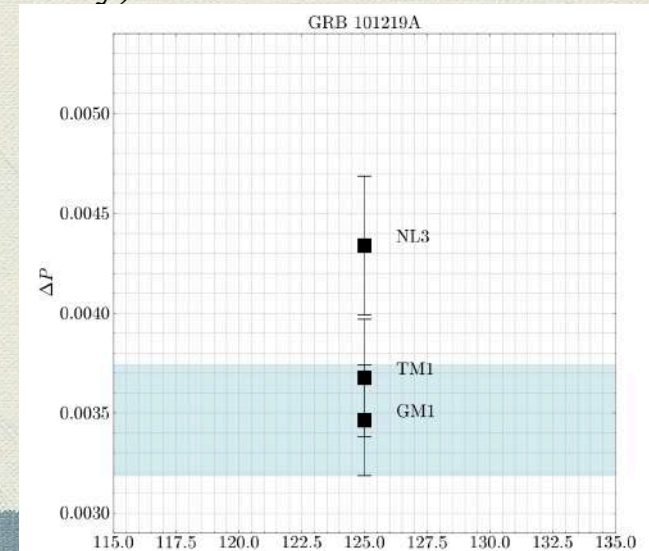
- - Lack of high quality data: GM1/TM1 degeneracy ($\sim 20\% \Delta\langle\Delta P\rangle$).
- - No exotic EOS (e.g., quark matter).
- - Limited to 3 nucleonic EOSs.

$$M_{\text{TOV}} \approx 2.3 \pm 0.1 M_{\odot}$$

$$M \geq M_{\text{crit}}(\alpha) = M_{\text{TOV}}(1 + kj^l)$$



20% $\Delta\langle\Delta P\rangle$



Toward a Multi-Messenger Probe of Dense Matter

- SGRB magnetar collapses offer a new probe into supranuclear matter EOS.
- Key Result: Intermediate EOS (GM1, $M_{\text{TOV}} \approx 2.4 M_{\text{sun}}$) preferred.

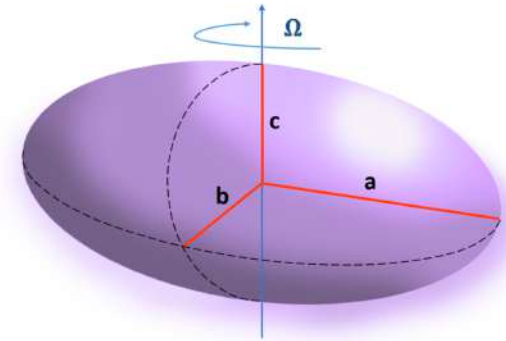
- Next Steps:

$$M_{\text{TOV}} \approx 2.3 \pm 0.1 M_{\odot}$$

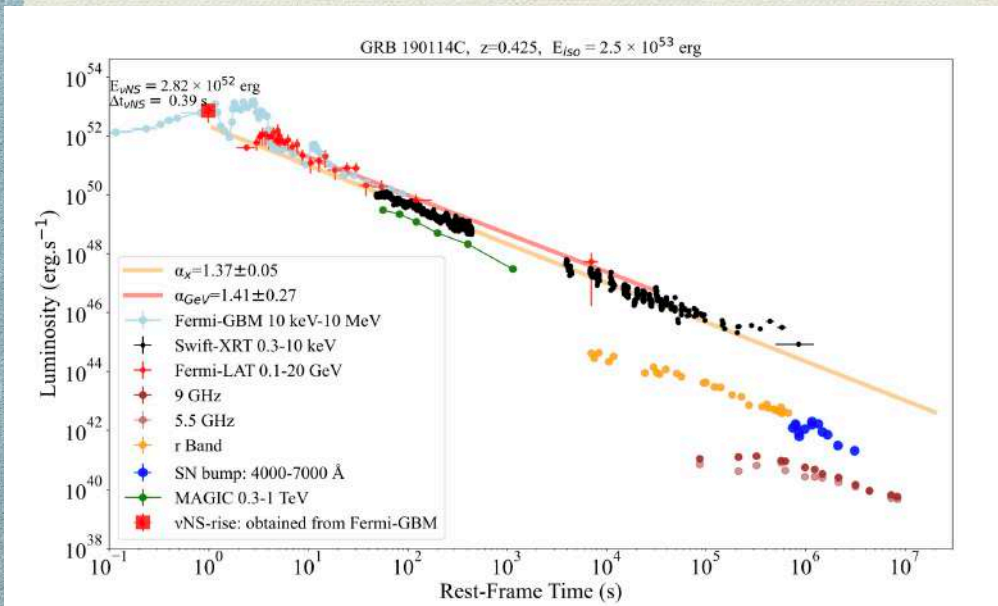
- Expand SGRB samples (e.g., Einstein Probe).
- Include hybrid/quark EOS, GW, accretion physics.
- Full GR simulations (e.g., RNS).
- Impact: Unifies electromagnetic and GW signals in EOS constraints.

Eccentricity of NS? GW Emission? Or Black hole??

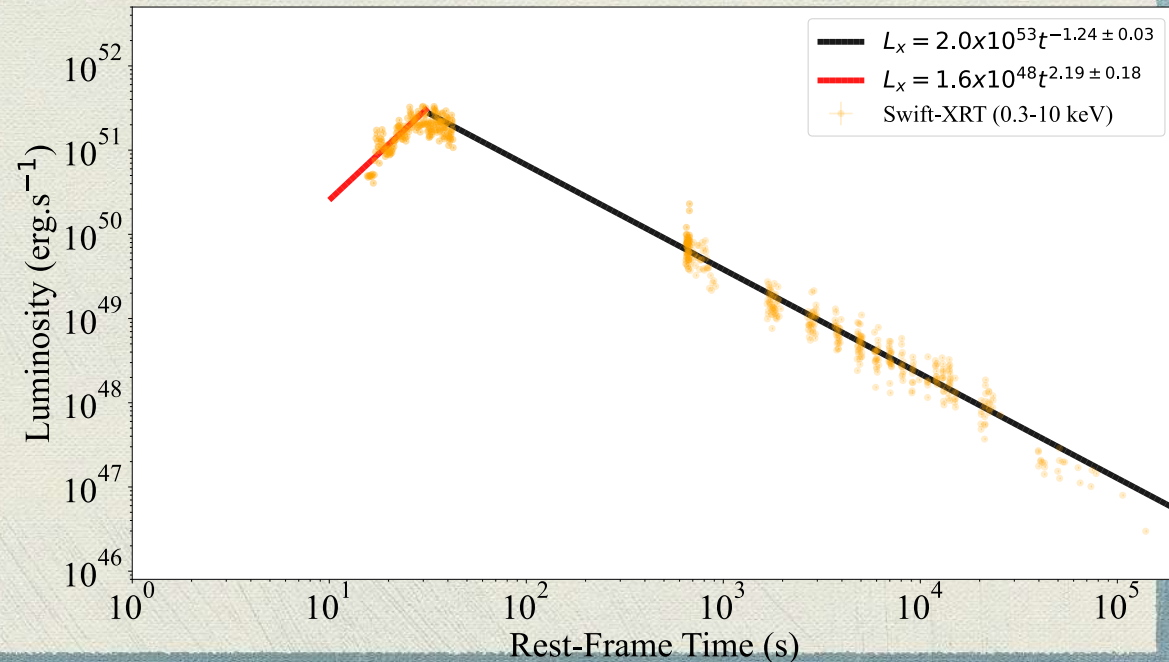
It is a newborn highly rotating NS,
Eccentricity is expected!



GRB 190114C



GRB 220101A



Multi-messenger signatures of a deformed magnetar in gamma-ray bursts

PARISA HASHEMI,¹ SOROUSH SHAKERI,^{1,2,3} YU WANG,^{4,5,6} LIANG LI,^{7,8,6} AND RAHIM MORADI⁹

¹Department of Physics, Isfahan University of Technology, Isfahan 84156-83111

²Iranian National Observatory, Institute for Research in Fundamental Sciences (IPM), P. O. Box 19395-5531 Tehran, Iran

³ICPAM, Isfahan, Isfahan University of Technology, Isfahan 84156-83111, Iran

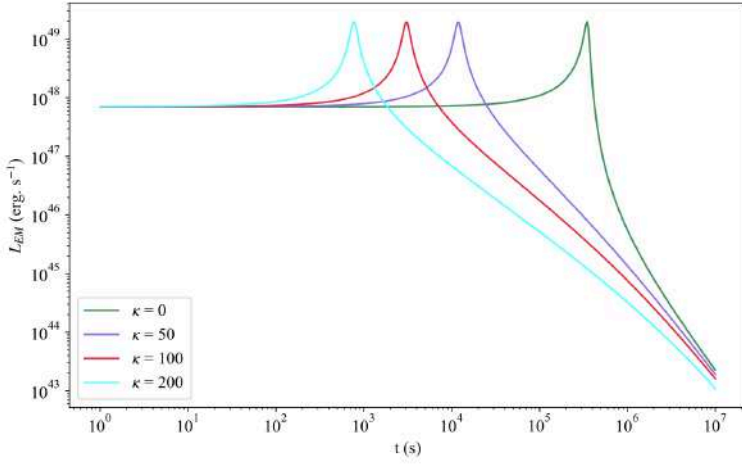


Figure 5. EM dipole and quadrupole emission of the compressible model with $\Gamma = 1.43$, $B = 10^{16}G$ and different fraction of dipole to quadrupole moments as labeled.

$$\frac{\dot{J}}{J} = \frac{1}{2} \left\{ \frac{g'}{g} + \frac{1}{3\Gamma - 4} \left[\frac{4(\Gamma - 1)e}{1 - e^2} - \frac{A'_3}{A_3} \right] \right\} \dot{e}.$$

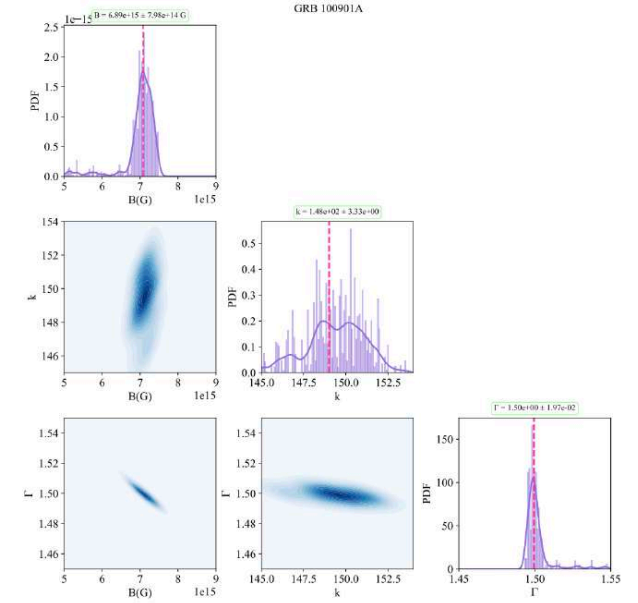
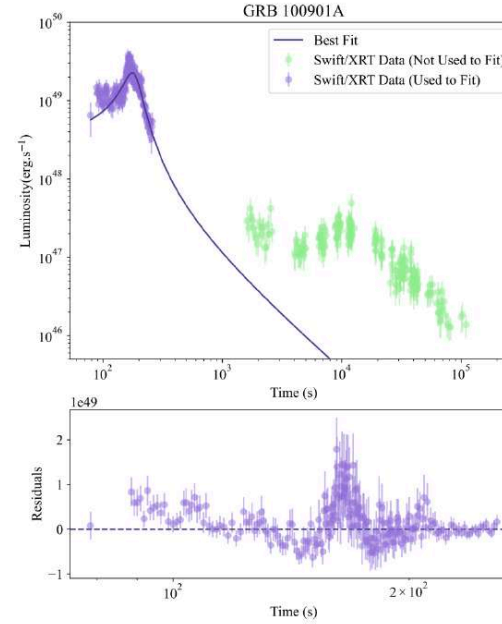
$$dE = \Omega dJ$$

$$A_3(e) = \frac{2}{e^2} \left[1 - (1 - e^2)^{1/2} \frac{\arcsin e}{e} \right].$$

$$P = K\rho^\Gamma,$$

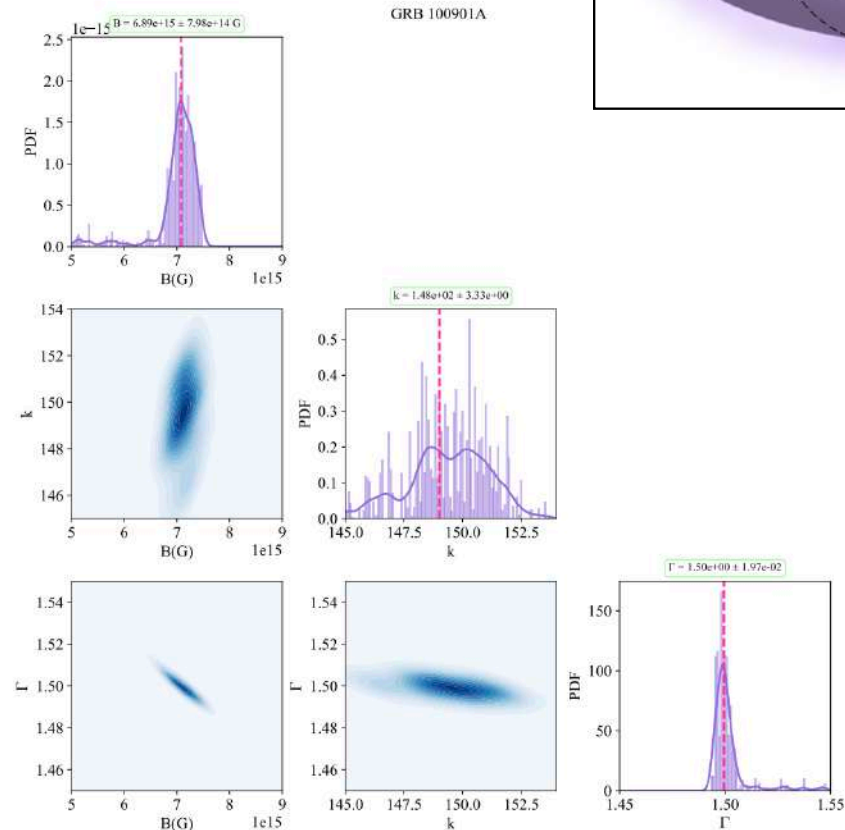
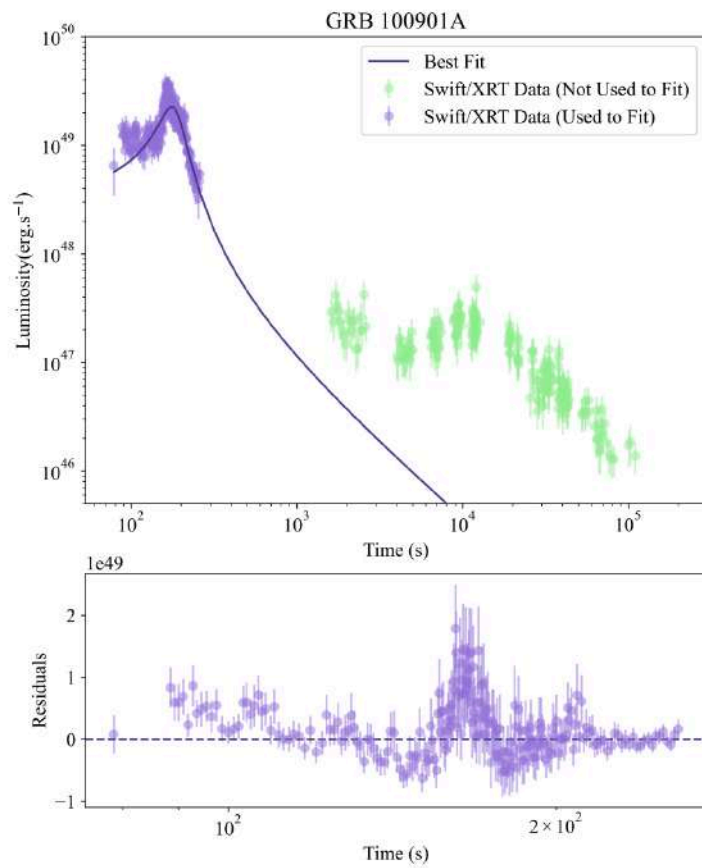
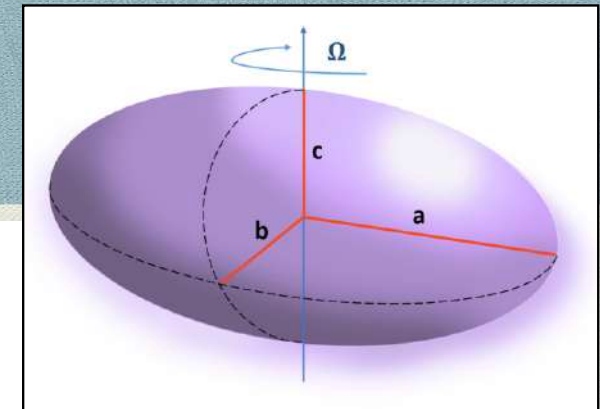
$$\dot{J}_{\text{EM}} = \dot{J}_{\text{dip}} + \dot{J}_{\text{quad}} = -\beta\Omega^3 - \xi\Omega^5.$$

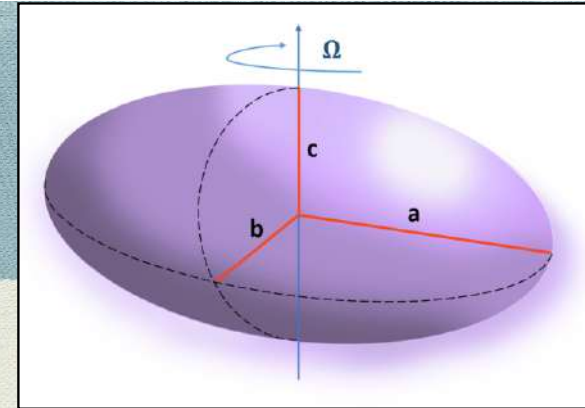
$$L_{\text{GW}} = -\dot{E}_{\text{GW}} = \frac{1}{5} \left\langle \frac{d^3 I_{jk}}{dt^3} \frac{d^3 I_{jk}}{dt^3} \right\rangle = \frac{32}{5} I^2 \epsilon^2 \Omega^6$$



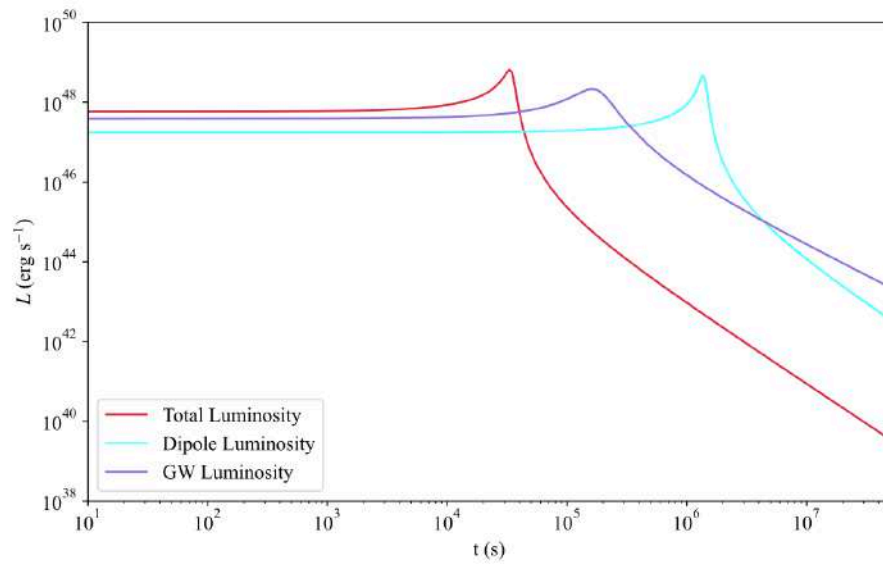
- Decreasing Eccentricity \rightarrow rapid drop in moment of inertia I
- Angular Momentum Loss $< I$ Drop $\rightarrow \Omega = J/I$ spikes
- Signature: brief X-ray flare in Swift-XRT light curve

X-ray flare; Compressible; Quadrupole EM

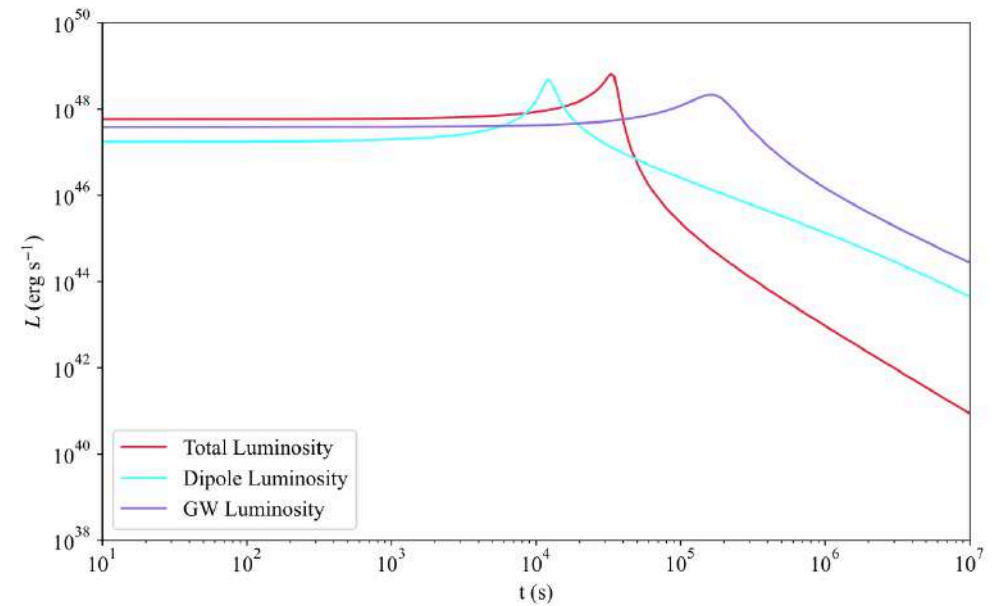


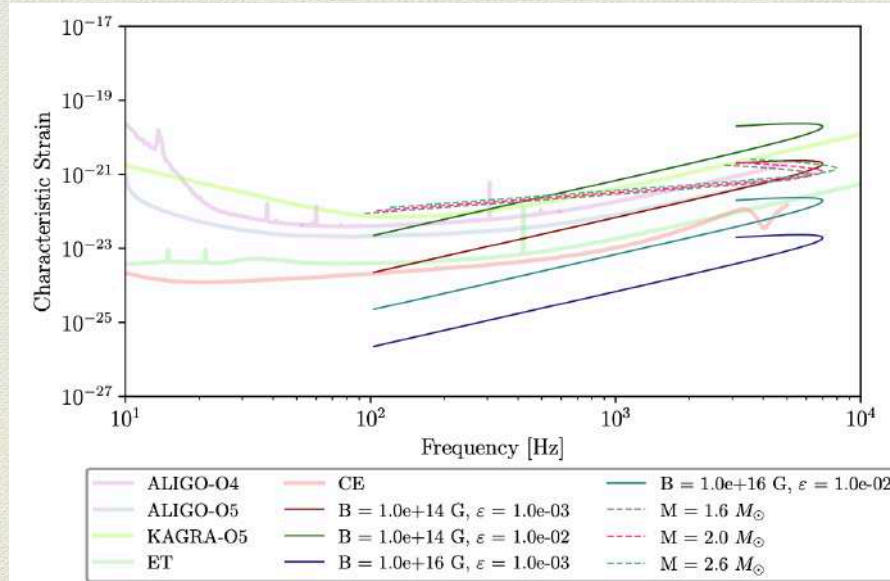
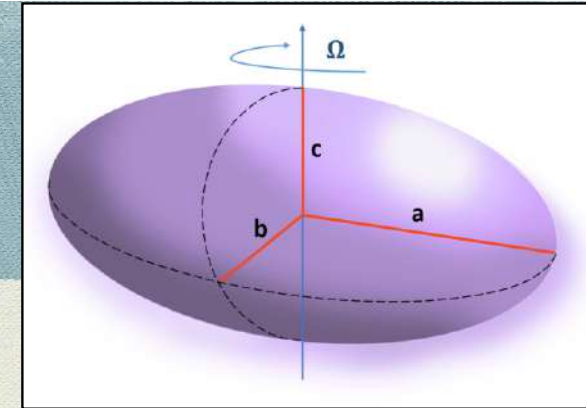


Compressible: Dipole+ GW



Compressible: Quadrupole EM + GW





Sensitivity and SNR values for different detectors.

GW Detector	$S(f_0 \approx 1 \text{ kHz})/\sqrt{Hz}$	SNR
ALIGO O4	5.75×10^{-24}	2.02
KAGRA O5	1.28×10^{-23}	0.93
ALIGO O5	2.53×10^{-24}	4.69
ET	5.76×10^{-25}	20.62
CE	3.27×10^{-25}	36.32

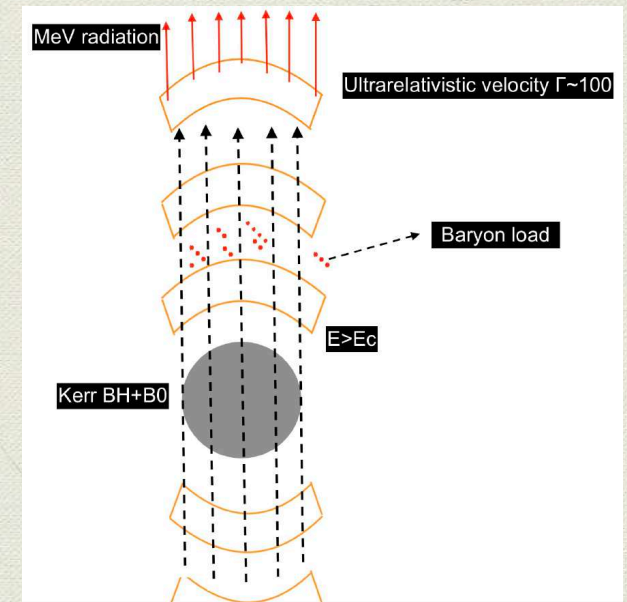
Conclusions

- Multipolar Magnetic field is successful in explaining the afterglow of GRBs
- Eccentricity is needed in explaining the afterglow evolution of energetic GRBs
- For having a more realistic solution: combine both and consider the proper Equation of state (EoS)
- $L = L_{\text{GW}} + L_{\text{dip}} + L_{\text{quad}} + \dots$
- *Numerical Solutions are needed to test different EoS
- *Proper EoS, in turn can explain the early flares activities in afterglow of GRBs and GW emission.

Conclusions and Perspective

- Most used model of LGRBs is Collapsar
- Formation of a BH is necessary in Collapsar model
- Two possibilities:
 - ★ 1. BH can behave like magnetar!
 - ★ 2. LGRBs' progenitor is a binary system!

Moradi et al., PRD104, 063043 (2021)



Similar idea for BH pulsar

The background features a series of overlapping, wavy, organic shapes in various shades of teal and dark blue. The shapes create a sense of depth and movement, resembling stylized mountains or flowing water. The colors transition from a deep navy blue at the top to lighter teal and greenish-blue towards the bottom.

Thank you!